NifS-Mediated Assembly of [4Fe−4S] Clusters in the N- and C-Terminal Domains of the NifU Scaffold Protein†

Archer D. Smith,‡ Guy N. L. Jameson,§ Patricia C. Dos Santos,|| Jeffrey N. Agar,‡ Sunil Naik,§ Carsten Krebs,§ Jeverson Frazzon,|| Dennis R. Dean,|| Boi Hanh Huynh,*,§ and Michael K. Johnson*,‡

Department of Chemistry and Center for Metalloenzyme Studies, University of Georgia, Athens, Georgia 30602, Department of Physics, Emory University, Atlanta, Georgia 30322, and Department of Biochemistry, Virginia Tech, Blacksburg, Virginia 24061

Received June 30, 2005; Revised Manuscript Received August 2, 2005

ABSTRACT: NifU is a homodimeric modular protein comprising N- and C-terminal domains and a central domain with a redox-active $[2Fe-2S]^{2+,+}$ cluster. It plays a crucial role as a scaffold protein for the assembly of the Fe−S clusters required for the maturation of *nif*-specific Fe−S proteins. In this work, the time course and products of *in vitro* NifS-mediated iron−sulfur cluster assembly on full-length NifU and truncated forms involving only the N-terminal domain or the central and C-terminal domains have been investigated using UV−vis absorption and Mössbauer spectroscopies, coupled with analytical studies. The results demonstrate sequential assembly of labile $[2Fe-2S]^{2+}$ and $[4Fe-4S]^{2+}$ clusters in the U-type N-terminal scaffolding domain and the assembly of $[4Fe-4S]^{2+}$ clusters in the Nfu-type C-terminal scaffolding domain. Both scaffolding domains of NifU are shown to be competent for *in vitro* maturation of nitrogenase component proteins, as evidenced by rapid transfer of $[4Fe-4S]^{2+}$ clusters preassembled on either the N- or C-terminal domains to the apo nitrogenase Fe protein. Mutagenesis studies indicate that a conserved aspartate (Asp37) plays a critical role in mediating cluster transfer. The assembly and transfer of clusters on NifU are compared with results reported for U- and Nfu-type scaffold proteins, and the need for two functional Fe−S cluster scaffolding domains on NifU is discussed.

Clusters of iron and inorganic sulfide are one of the most common and functionally diverse types of prosthetic groups in all of biology, with roles ranging from electron transfer and catalysis to sensing and regulation (*1*, *2*). Moreover, the importance of this class of protein prosthetic group has generated considerable interest in understanding how they are fabricated within the cell. Major progress has been made in the past decade in understanding the complex process of Fe−S cluster biosynthesis using both *in vivo* and *in vitro* approaches (for recent reviews see refs *3*−*6*). Three distinct types of biosynthetic machinery have emerged, termed NIF (nitrogen fixation) (*7*), ISC (iron−sulfur cluster) (*8*), and SUF (sulfur utilization factor) (*9*). However, following the model originally established for the NIF system (*10*, *11*), each is believed to use a similar overall mechanism involving pyridoxal phosphate (PLP)[1]-dependent cysteine desulfurases (NifS/IscS/SufS) that supplies the inorganic sulfur for the biosynthesis of [2Fe−2S] or [4Fe−4S] clusters on a variety of scaffold proteins (NifU/IscU/SufU, ^{Nif}IscA/IscA/SufA, and Nfu type). The preassembled clusters are generally believed to be transferred intact into apo Fe−S proteins, but thus far, this transfer has only been well-documented for [2Fe−2S] clusters (*12*−*16*).

The NIF system comprises NifS, NifU, and ^{Nif}IscA (*10*, *11*, *17*, *18*) and functions primarily for the assembly of Fe−S clusters to be used in the maturation of the nitrogenase component proteins and hence is present in nitrogen-fixing bacteria. However, other NifS- and NifU-like proteins can also function in general Fe−S cluster biosynthesis in prokaryotes and eukaryotes, as evidenced by characterization of NifS and NifU homologues in nondiazotrophic bacteria, such as *Helicobacter pylori* (*19*), and in the anaerobic, amitochondrial protozoan parasite, *Entamoeba histolytica* (*20*). The ISC system is composed of IscS, IscU, IscA, Fdx (a [2Fe−2S] Fd), and two heat-shock cognate proteins, HscA and HscB (*8*, *21*). This type of assembly machinery is very widespread, and partial or complete sets of the ISC components are conserved from bacteria to higher eukaryotes (*3*−*6*). Moreover, the involvement of HscA and HscB in the ISC system is particularly intriguing, because they exhibit ATPase activity and high-sequence homology to the family of molecular chaperones represented by the DnaK and DnaJ partner proteins. HscA and HscB have been shown to act in concert to bind IscU (*22*−*25*) and are proposed to facilitate cluster transfer from IscU to acceptor proteins in an ATP-dependent process (*26*). The SUF system comprises SufA, SufU, SufB, SufC, SufD, SufS, and SufE and is found, in whole or in part, in a wide range of bacteria, archaea and

† This work was supported by grants from the National Institutes of Health (GM62542 to M.K.J. and GM47295 to B.H.H.) and the National Science Foundation (MCB-021138 to D.R.D.).

* To whom correspondence should be addressed. Telephone: 404-727-4295. Fax: 404-727-0873. E-mail: vhuynh@emory.edu (B.H.H.); Telephone: 706-542-9378. Fax: 706-542-2353. E-mail: johnson@chem.uga.edu (M.K.J.).

‡ University of Georgia.

§ Emory University.

|| Virginia Tech.

[1] Abbreviations: DTT, dithiothreitol; PMSF, phenyl methyl sulfonyl fluoride; PLP, pyridoxal phosphate.

10.1021/bi051257i CCC: $30.25
Published on Web 09/10/2005

Scheme 1: Primary Sequence and Modular Organization of *A. vinelandii* NifU[a]

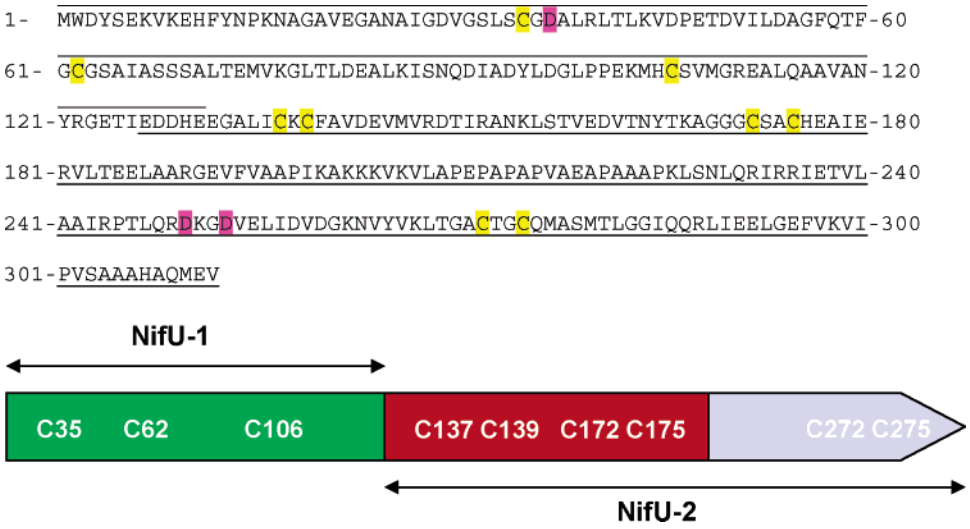

[a] Conserved cysteine and aspartate residues that are potential cluster ligands are highlighted in yellow and purple, respectively. Residues corresponding to NifU-1 and NifU-2 are overlined and underlined, respectively. The N-terminal, central, and C-terminal domains of NifU are indicted in green, red, and lilac, respectively.

plastids (*4*, *9*, *27*). SufBCD constitutes an unorthodox ATPase related to the ABC superfamily that stimulates the cysteine desulfurase activity of SufS, along with SufE (*28*, *29*). SufE has recently been shown to have structural homology with IscU (*30*, *31*) and to function as a sulfurtransferase that facilitates transfer of sulfane sulfur (S^0) from SufS to acceptor proteins (*29*, *32*). On the basis of the composition of operons (*4*, *9*) or *in vitro* studies (*33*, *34*), SufA or SufU are likely to provide scaffold proteins for the SUF machinery in many organisms, but both are absent in many archaea that contain SufBCD (*9*).

Thus far, three distinct types of Fe−S cluster scaffold proteins with distinct arrangements of cluster-ligating cysteine residues have been identified on the basis of sequence homology and *in vitro* cluster assembly and/or transfer studies, and each has been shown to be able to accommodate $[2Fe-2S]^{2+}$ or $[4Fe-4S]^{2+}$ clusters. The A-type motif found in ^{Nif}IscA, IscA, and SufA has three conserved cysteine residues in a C-X_{61-65}-C-X-C arrangement that is common to all three cluster assembly machineries. *In vitro* cluster assembly studies have provided evidence for assembly of $[2Fe-2S]^{2+}$ and $[4Fe-4S]^{2+}$ clusters on *Azotobacter vinelandii* ^{Nif}IscA (*18*, *35*) and *Erwinia chrysantemi* SufA (*33*) and $[2Fe-2S]^{2+}$ clusters on IscA (Isa in eukarya) proteins from *Escherichia coli* (*13*), *Schizosaccharomyces pombe* (*15*, *36*), and *Synechocystis* (*16*, *37*).

The U-type motif is found at the N terminus of NifU, as well as in IscU (Isu in eukarya), and comprises three conserved cysteine residues in a C-X_{24-26}-C-X_{42-43}-C arrangement. SufUs are homologous to IscUs with the same three conserved cysteine residues, but they have some distinguishing characteristics (*4*): an 18−21 amino acid insert between the second and third conserved cysteine residues; a conserved lysine in place of the conserved histidine that coordinates Zn in the NMR structure of *Haemophilis influenzae* IscU, along with the three conserved cysteine residues (*30*); absence of the LPPVK motif that is required to interact with HscA cochaperone (*25*). Hence, in contrast to IscU, it seems likely that SufU does not require HscA/HscB cochaperones for Fe−S cluster assembly or transfer. In addition, the differences in primary structure for SufU compared to IscU are likely responsible for differences in the reported NMR structures. *Thermatoga maritima* SufU is reported to have a molten globule-type structure that lacks a well-defined ternary structure (*38*, *39*), whereas *H. influenzae* IscU has a well-defined central core that includes the Fe−S cluster-binding region (*30*). *In vitro* cluster assembly studies have shown sequential assembly of $[2Fe-2S]^{2+}$ and $[4Fe-4S]^{2+}$ clusters on *Av* IscU (*40*) and assembly of $[2Fe-2S]^{2+}$ clusters on the N-terminal fragment of *Av* NifU (NifU-1) (*11*), IscU, or Isu proteins from *E. coli* (*41*), *S. pombe* (*42*), and *Homo sapiens* (*14*, *43*) and SufU from *T. maritima* (*34*).

The third motif is found in the C-terminal domain of NifU, as well as in the "NifU-like" proteins termed Nfu or CnfU (for chloroplast NifU-like), and comprises a conserved C-X_2-C motif. Absorption studies have provided evidence for a $[2Fe-2S]^{2+}$ cluster in the as-purified Nfu protein from *Synechocystis* (*12*, *44*), and the combination of absorption, analytical, and Mössbauer studies has demonstrated the assembly of a $[4Fe-4S]^{2+}$ cluster on the human Nfu protein (*45*).

The homodimeric NifU protein is unique among scaffold proteins in having a modular structure (*46*) comprising three distinct domains (see Scheme 1), two of which are potential sites for cluster assembly; an IscU-type domain at the N terminus that utilizes conserved residues C37, C62, and C106 in *Av* NifU and an Nfu-type site at the C terminus that utilizes conserved residues C272 and C275 in *Av* NifU. Indeed, recent genetic and biochemical studies indicate that both the N- and C-terminal domains are functional in mediating assembly of the [4Fe−4S] cluster on apo nitrogenase Fe protein (*47*). In addition, the central domain of NifU contains a permanent, redox-active $[2Fe-2S]^{2+,+}$ cluster ligated by residues C137, C139, C172, and C175 in *Av* NifU (*46*, *48*) with sequence homology to the bacterioferritin-associated *E. coli* [2Fe−2S] ferredoxin (*49*, *50*). The role of the permanent $[2Fe-2S]^{2+,+}$ cluster has yet to be determined but is likely to play a redox role in recruiting Fe for cluster assembly or in mediating the cluster assembly or release

processes. However, *in vitro* studies of NifS-mediated cluster assembly involving NifU have thus far been confined to the isolated N-terminal (IscU-like) domain of *Av* NifU (termed NifU-1, see Scheme 1), variants of NifU-1 in which a $[2Fe-2S]^{2+}$ cluster is stabilized via a D37A mutation, and full-length *Av* NifU that is deficient in the permanent clusters as a result of C137A mutation. Hence, there is a pressing need to investigate the mechanism and type of clusters that can be assembled on full-length wild-type NifU and to establish how NifU facilitates cluster incorporation and maturation of nitrogenase proteins.

We report here a spectroscopic investigation of the time course and products of NifS-mediated cluster assembly on wild-type NifU, wild-type and D37A NifU-1 (N-terminal domain fragment of NifU), and wild-type NifU-2 (central plus C-terminal domain fragments of NifU) (see Scheme 1). The approach involves analytical, UV−vis absorption, and Mössbauer studies, with particular emphasis on the use Mössbauer to address the nature of assembled clusters via NifS-mediated reconstitution of natural abundance or ^{57}Fe-enriched NifU samples in the presence of added ^{57}Fe. The results indicate that *Av* NifU can sequentially assemble labile $[2Fe-2S]^{2+}$ and $[4Fe-4S]^{2+}$ clusters in the N-terminal (IscU-type) domain and labile $[4Fe-4S]^{2+}$ clusters in the C-terminal (Nfu-type) domain. Moreover, we demonstrate that $[4Fe-4S]^{2+}$ clusters preassembled in either the N- or C-terminal domains can be rapidly transferred to apo nitrogenase Fe protein, indicating that both scaffolding domains of NifU are competent for maturation of nitrogenase component proteins.

MATERIALS AND METHODS

DNA Biochemistry, Plasmids, and Strain Constructions. The construction of plasmids used for the heterologous expression of NifU, NifU-1, D37A NifU-1, and NifU-2 has been previously described (*11*, *46*, *48*). The poly-histidine tagged *nifS* gene was engineered by PCR to contain *Nde*I and *Bam*HI sites and ligated into pT_7-7 *Nde*I−*Bam*HI sites. The poly-histidine tag (seven histidines) is located near the C-terminal domain inserted into a *Sma*I−*Stu*I deletion and has been shown to retain full physiological function by genetic rescue experiments. The $nifS_{his7}$ pDB845 plasmid is ampicillin-resistant.

Protein Biochemistry. Av NifU (pDB525) was heterologously overexpressed in *E. coli* strain BL21(DE3) as previously described (*48*). Typical purifications utilized 80−120 g of *E. coli* cells that were resuspendend (1:3, w/v) in 50 mM Tris/HCl buffer at pH 7.4, with the buffer containing 2 mM β-mercaptoethanol and both RNAse and DNAse (Promega, 3.75 mg/L) in addition to 0.5% (w/v) phenylmethanesulfonyl fluoride (PMSF) (Sigma). After sonication and centrifugation, the soluble cell-free extract was decanted and NifU was subsequently precipitated at 33% ammonium sulfate saturation. The precipitated NifU pellet was resuspended in zero salt buffer, loaded onto a Q Sepharose (Pharmacia) column (50 mm inner diameter, ∼80 mL), and washed with 5 column volumes at 0.1 M NaCl before eluting with 0.1−0.6 M NaCl linear gradient over 600 mL. Fractions containing NifU were collected between 0.27 and 0.34 M NaCl and pooled as a single fraction. *Av* $NifS_{his7}$ was heterologously expressed in *E. coli* strain BL21(DE3) as previously described (*10*). $NifS_{his7}$-containing cells were resuspended in 50 mM Tris/HCl buffer at pH 8.0, with the buffer containing 5 mM imidazole, 500 mM NaCl, DNAse (Promega, 3.75 mg/L), RNAse (Promega, 3.75 mg/L), and 0.5% PMSF, sonicated, centrifuged, and retaining the soluble cell-free extract. The cell-free extract was loaded onto a Ni^{2+}-charged 5-mL HiTrap (Pharmacia) metal-chelating column and washed with 10 column volumes of 50 mM Tris/HCl buffer at pH 8.0 containing 60 mM imidazole and 500 mM NaCl. $NifS_{his6}$ was eluted with 50 mM Tris/HCl buffer at pH 8.0, with 1 M imidazole and 500 mM NaCl, and immediately loaded onto a 53-mL HiPrep (Pharmacia) desalting column equilibrated with 100 mM Tris/HCl buffer at pH 7.8, with 100 mM NaCl, to remove the imidazole. *Av* NifU-1, D37A NifU-1, and NifU-2 were purified as previously described (*11*, *46*). All samples of NifS, NifU, and NifU variants were at least >95% homogeneous based on denaturing sodium dodecyl sulfate−polyacrylamide gel electrophoresis (SDS−PAGE).

Preparation of NifU Samples for NifS-Mediated Cluster Assembly Experiments. Iron and protein content of wild-type *Av* NifU determined after purification typically ranged from 1.1 to 1.5 Fe/NifU monomer, significantly less than the 2.0 Fe/NifU monomer expected for 1 permanent $[2Fe-2S]^{2+,+}$ cluster/NifU monomer. The substoichiometric cluster occupancy is most likely an artifact of either overexpression or cluster degradation during purification. Because substoichiometric occupancy of permanent clusters would complicate the interpretation of NifS-mediated cluster assembly studies, the following procedures were used to obtain NifU samples with fully replete natural abundance or ^{57}Fe-enriched permanent clusters for NifS-mediated cluster assembly studies. Both procedures were carried out in a glovebox under argon (<5 ppm O_2).

Samples of wild-type NifU as purified with natural abundance Fe were incubated with catalytic amounts of NifS (NifS/NifU ratio of 1:35) in the presence of a 20-fold excess of dithiothreitol (DTT), a 40-fold excess of L-cysteine, and a 10-fold excess of natural abundance Fe^{2+}. After reconstitution, samples of NifU were re-isolated from the reconstitution mixture by loading the reconstitution cocktail onto a Q-sepharose column, washing with 10 column volumes of 0.15 M NaCl, and eluting NifU with 0.50 M NaCl in a single fraction. After reisolation, NifU samples were incubated with a 10-fold excess of dithionite and a 40-fold excess of EDTA for 30 min to remove any transient Fe−S clusters and adventitiously bound iron. Excess dithionite and EDTA were removed using a 53-mL HiPrep (Pharmacia) desalting column equilibrated 100 mM Tris/HCl buffer at pH 7.8, with 0.1 M NaCl. Samples were oxidized with excess thionine in the presence of 2 mM DTT and again repurified using the HiPrep desalting column prior to use in NifS-mediated cluster assembly experiments. The resulting NifU samples had permanent $[2Fe-2S]^{2+,+}$ cluster occupancy greater than 90% based on iron and protein determinations that were in the range of 1.8−2.1 Fe/monomer and had A_{460}/A_{277} ratios ≥0.31. Average extinction coefficients for the oxidized $[2Fe-2S]^{2+}$ cluster in these NifU samples were $\epsilon_{460} = 9.1$ mM^{-1} cm^{-1} and $\epsilon_{277} = 28$ mM^{-1} cm^{-1}. The same procedure was not performed for NifU-2, because samples were purified with permanent clusters ≥85% intact as evidenced by Fe analyses

(1.7−1.8 Fe/monomer) and UV−vis absorption properties ($\epsilon_{460} = 8.0$ mM^{-1} cm^{-1}, $\epsilon_{280} = 10.9$ mM^{-1} cm^{-1}).

Samples of NifU with ^{57}Fe-enriched permanent clusters were prepared by acid denaturation of NifU and reconstitution of the permanent clusters on apo NifU using ^{57}Fe. As purified NifU, ~0.1 mM in 50 mM Tris/HCl buffer at pH 8, with 5.0 mM DTT, 0.2 M NaCl, and 10.0 mM α-α′-bipyridyl, was slowly acidified by dropwise addition of HCl with continuous stirring until the solution reached approximately pH 3.0. Once the solution changed from a brown to a cherry red color, indicating the formation of apo-NifU and chelation of the free iron, the pH was slowly raised to pH 7.8 by buffer exchange with 100 mM Tris/HCl buffer at pH 7.8 containing 5.0 mM DTT and 0.2 M NaCl and repurified using a 53-mL HiPrep desalting column equilibrated with 100 mM Tris/HCl buffer at pH 7.8, with 0.1 M NaCl. Samples of NifU replete with ^{57}Fe-enriched permanent clusters were prepared by reconstitution of apo-NifU using $^{57}Fe^{2+}$, using the same procedure as that described above for reconstitution of permanent clusters with natural abundance Fe^{2+}.

NifS-Mediated Cluster Assembly on NifU. All samples of full-length and truncated forms of NifU were pretreated with DTT (incubated with 2 mM DTT, which was subsequently removed by anaerobic gel filtration prior to use), and NifS-mediated cluster assembly studies were carried out under an argon atmosphere (<5 ppm O_2) in a Vacuum Atmospheres glovebox. The cluster assembly reaction mixture comprised full-length or truncated forms of NifU (NifS/NifU ratio of 1:35), L-cysteine (32-fold excess/NifU monomer) and Fe^{2+} (8−25-fold excess of either natural abundance Fe or ^{57}Fe/NifU monomer) in a 100 mM Tris/HCl buffer at pH 7.8, with 0.1 M NaCl. Anion-exchange chromotography was employed to repurify full-length and truncated forms of NifU, following NifS-mediated cluster assembly. The reaction mixture was loaded onto a 5-mL High-Trap Q-sepharose (Pharamacia) column and washed with 5 column volumes of 0.1 M NaCl buffer and 5 column volumes of 0.15 M NaCl buffer, before eluting in a single fraction with buffer containing 0.5 M NaCl.

Chemical Analysis. Protein concentrations were determined using the BioRad D_c protein assay in conjunction with the microscale modified procedure of Brown et al. (*51*), with BSA as a standard (Roche). Iron determinations were performed after $KMnO_4$/HCl protein digestion as described by Fish (*52*) and Ugulava et al. (*53*), using a 1000 ppm atomic absorption iron standard (Spectrum) as the reference.

Preparation of Nitrogenase Apo-Fe Protein. Av nitrogenase Fe protein was isolated from *A. vinelandii* cells grown under diazatrophic conditions and purified as previously described (*47*). Removal of the [4Fe−4S] cluster was carried out by incubating Fe protein in the presence of 10 mM ATP, 30 mM $MgCl_2$, 20 mM sodium dithionite, and 20 mM α-α′-bipyridyl in a sealed vial at 4 °C for 3 h. The apo-Fe protein was subsequently purified by loading the apo-Fe protein cocktail onto a G-25 sephadex column equilibrated with 50 mM Tris/HCl buffer at pH 7.8 containing 5.0 mM ATP, 15 mM $MgCl_2$, and 0.15 M NaCl and eluting with the same buffer.

Apo-Fe Protein Reactivation Assay. Apo-Fe protein reactivation assays were carried out by adding NifU or NifU variants (1−4-fold molar excess of dimeric NifU) with spectroscopically and analytically defined cluster contents to a solution containing 5.6 μM dimeric apo-Fe protein in 25 mM Tris/HCl buffer at pH 7.4, with 4 mM DTT and 4 mM MgATP under an argon atmosphere. The cocktail was assayed immediately using the nitrogenase hydrogen evolution assay as described previously (*47*). Assay vials contained 0−11.2 nmol of dimeric NifU or NifU variants, 2.8 nmol of dimeric Fe-protein, and 1.4 nmol of tetrameric MoFe protein in 1 mL. Samples were incubated at 30 °C, in duplicate, for 20 min before quenching the reaction with 50 mM EDTA and quantifying the hydrogen gas produced using a Shimadzu GC-14 chromatograph equipped with a molecular sieve 5A column and thermal conductivity detector. The individual measurements differed by less that 5%, and the data presented are the average of the two measurements.

Spectroscopic Methods. Samples for all spectroscopic investigations were prepared under an argon atmosphere in a Vacuum Atmospheres glovebox (<5 ppm O_2). UV−vis absorption spectra were recorded in sealed anaerobic 1 mm quartz cuvettes, using a Shimadzu 3101PC scanning spectrophotometer. Mössbauer spectra were recorded by using the previously described instrumentations (*54*). The zero velocity of the spectra refers to the centroid of a room-temperature spectrum of a metallic Fe foil. Analysis of the Mössbauer data was performed with the WMOSS program (Web Research).

RESULTS

NifS-Mediated Cluster Assembly on Wild-Type NifU. The time course and products of NifS-mediated Fe−S cluster assembly on wild-type NifU were monitored by UV−vis absorption and Mössbauer spectroscopies. Catalytic amounts of NifS were used to slow the cluster assembly process and minimize the contribution of the NifS PLP chromophore to the UV−vis absorption spectrum. The absorption spectrum of NifU comprises a protein band centered at 280 nm and S-to-Fe charge-transfer transitions from the permanent $[2Fe-2S]^{2+}$ cluster throughout the UV−vis region (*48*) (see Figure 1, - - -). NifS-mediated cluster assembly, using an 8-fold stoichiometric excess of Fe^{2+} ion, is evident by a gradual increase in the UV−vis absorption over a period of 2 h, with the most pronounced changes occurring in the first 40 min (see Figure 1). After 2 h of NifS-mediated cluster assembly, repurification of NifU using anaerobic anion-exchange chromatography shows that cluster assembly has indeed occurred on NifU and subtraction of the original NifU absorption spectrum reveals the UV−vis absorption characteristics of the assembled Fe−S cluster(s) (see inset of Figure 1). The resultant absorption spectrum has a pronounced shoulder centered at 400 nm ($\epsilon_{400} = 15$ mM^{-1} cm^{-1}) that is characteristic of the assembly of approximately 1 $[4Fe-4S]^{2+}$ cluster/NifU monomer. Moreover, analytical data indicated the presence of 6.1 Fe/NifU monomer, consistent with the presence of 1 permanent $[2Fe-2S]^{2+}$ cluster and 1 assembled $[4Fe-4S]^{2+}$ cluster. This result was initially surprising in light of the UV−vis absorption and resonance Raman evidence for the assembly of a $[2Fe-2S]^{2+}$ cluster on the IscU-like N-terminal fragment of NifU (NifU-1) and the D37A variant of full-length NifU (*11*). Hence, parallel Mössbauer studies were carried out to provide a more discriminating means of assessing the clusters assembled on NifU as a result of NifS-mediated cluster assembly.

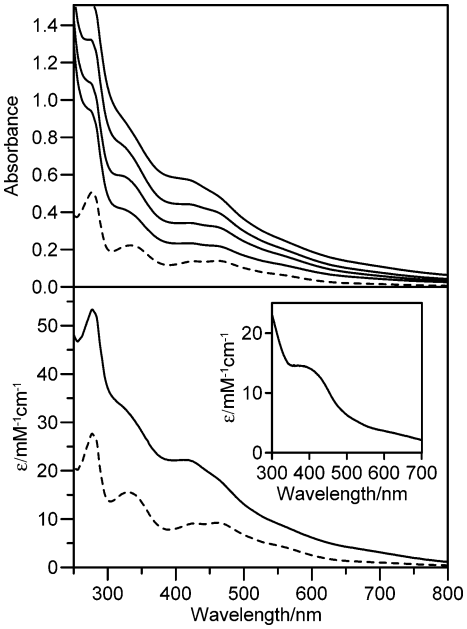

FIGURE 1: NifS-mediated assembly of Fe−S clusters on wild-type *A. vinelandii* NifU monitored by UV−vis absorption. (Top) Time course of NifS-mediated cluster assembly on NifU. The dashed line is NifU prior to addition of NifS, cysteine, and Fe^{2+} ion, and the solid lines are spectra of the reaction mixture recorded at 10, 20, 30, and 40 min after initiating NifS-mediated cluster assembly (absorbance increasing with increasing time). The reaction mixture consisted of 182 μM NifU, 4.2 μM NifS, 1.5 mM Fe^{2+}, and 6 mM L-cysteine. (Bottom) Purified NifU before and after NifS-mediated cluster assembly. The dashed line is NifU before NifS-mediated cluster assembly, and the solid line is NifU after NifS-mediated cluster assembly for 2 h and repurification using Q-sepharose anion-exchange chromatography. The inset shows the difference spectrum corresponding to purified NifU after minus before NifS-mediated cluster assembly.

Mössbauer spectra of ^{57}Fe-enriched wild-type NifU before and after 2 h of NifS-mediated cluster assembly using a 14-fold excess of $^{57}Fe^{2+}$ and repurification using anaerobic anion-exchange chromatography, are shown in parts A and B of Figure 2, respectively. Prior to NifS-mediated cluster assembly, the Mössbauer spectrum (Figure 2A) is dominated (92% of the total intensity) by the quadrupole doublet (shown in brown) of an $S = 0$ $[2Fe-2S]^{2+}$ cluster, which is composed of 2 antiferromagnetically coupled high-spin Fe^{3+} sites ($\Delta E_Q = 0.59$ mm/s and $\delta = 0.27$ mm/s for site 1, and $\Delta E_Q = 0.37$ mm/s and $\delta = 0.28$ mm/s for site 2, see Table 1) and has a small contribution (8% of the total intensity) from a $S = {}^1/_2$ $[2Fe-2S]^{+}$ cluster. Hence, the Mössbauer spectrum of wild-type NifU exclusively arises from the permanent $[2Fe-2S]^{2+,+}$ cluster and, taken together with Fe determinations (2.0 Fe/NifU monomer), confirms the presence of 1 permanent $[2Fe-2S]^{2+,+}$ cluster/NifU monomer. The Mössbauer spectrum of the repurified NifU after NifS-mediated cluster assembly reveals 2 quadrupole doublets in a 2:1 ratio (Figure 2B). The less intense doublet (shown in brown) is identical to that of the permanent $[2Fe-2S]^{2+}$ cluster that was present prior to NifS-mediated clusters assembly, and the more intense doublet (shown in blue) is characteristic of $S = 0$ $[4Fe-4S]^{2+}$ clusters comprising 2 valence-delocalized $Fe^{2+}Fe^{3+}$ pairs. The parameters determined for the $[4Fe-4S]^{2+}$ cluster in the repurified NifU are $\Delta E_Q = 1.29$ mm/s and $\delta = 0.47$ mm/s for pair 1 and $\Delta E_Q = 1.00$ mm/s and $\delta = 0.45$ mm/s for pair 2 (see Table 1).

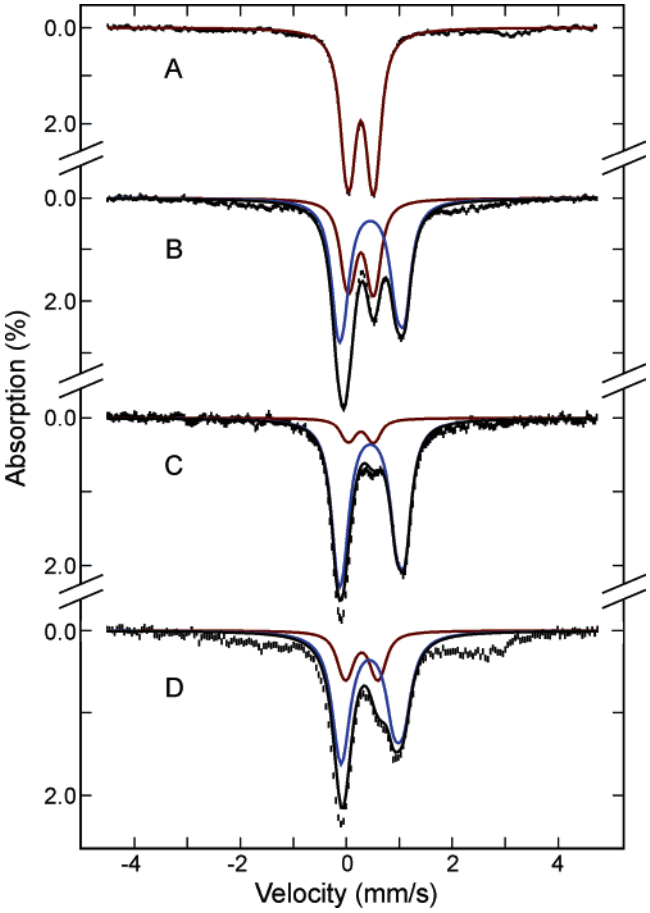

FIGURE 2: Mössbauer spectra of purified NifU samples recorded at 4.2 K with a parallel applied field of 50 mT. (A) ^{57}Fe-enriched wild-type NifU (1.02 mM). (B) ^{57}Fe-enriched wild-type NifU (0.49 mM) after NifS-mediated cluster assembly using $^{57}Fe^{2+}$. (C) Natural abundance NifU-2 (0.21 mM) after NifS-mediated cluster assembly using $^{57}Fe^{2+}$. (D) NifU-1 (0.45 mM) after NifS-mediated cluster assembly using $^{57}Fe^{2+}$. Brown, $[2Fe-2S]^{2+}$ clusters; blue, $[4Fe-4S]^{2+}$ clusters; black, composite simulations of the central quadrupole doublets. Parameters used in the simulations are listed in Table 1.

When the Mössbauer absorption intensities determined for the 2 clusters are taken together with the analytical data of 5.3 Fe/NifU monomer obtained for this sample, they (34% for the $[2Fe-2S]^{2+}$ and 60% for the $[4Fe-4S]^{2+}$ cluster) indicate the presence of approximately 0.8 $[4Fe-4S]^{2+}$ and 0.9 $[2Fe-2S]^{2+}$ clusters/NifU monomer, in good agreement with the UV−vis absorption data.

Mössbauer studies also afford insight into the time course of the NifS-mediated cluster assembly process. Mössbauer spectra of the reaction mixture at selected time points during NifS-mediated cluster assembly on ^{57}Fe-enriched wild-type NifU using a 22-fold excess of $^{57}Fe^{2+}$ are shown in the top of Figure 3. Global analysis of the data indicates quadrupole doublets from five spectral components. Three components correspond to monomeric high-spin Fe^{2+} species (shown in green) with parameters similar to those previously characterized for reaction mixtures during NifS-mediated cluster assembly on ^{Nif}IscA (*18*). The other two components are quadrupole doublets indicative of $S = 0$ $[2Fe-2S]^{2+}$ clusters (shown in brown) and $S = 0$ $[4Fe-4S]^{2+}$ clusters (shown in blue). The parameters obtained for the Fe−S clusters observed during assembly are similar but not identical to those determined for the permanent $[2Fe-2S]^{2+}$ cluster and

Table 1: Mössbauer Parameters for the Fe−S Clusters in Purified NifU Samples before and after NifS-Mediated Cluster Assembly with $^{57}Fe^{2+}$

sample	cluster type	δ (mm/s)[a]	ΔE_Q (mm/s)[a]	line width (mm/s)
^{57}Fe-enriched NifU	$[2Fe-2S]^{2+}$			
before cluster assembly	site 1	0.27	0.59	0.27
	site 2	0.28	0.37	0.27
^{57}Fe-enriched NifU	$[2Fe-2S]^{2+}$			
after cluster assembly	site 1	0.27	0.59	0.27
	site 2	0.28	0.37	0.27
	$[4Fe-4S]^{2+}$			
	pair 1	0.47	1.29	0.29
	pair 2	0.45	1.00	0.32
natural-abundance NifU-2	$[2Fe-2S]^{2+}$			
after cluster assembly	site 1	0.27	0.59	0.27
	site 2	0.28	0.37	0.27
	$[4Fe-4S]^{2+}$			
	pair 1	0.47	1.29	0.29
	pair 2	0.45	1.00	0.32
NifU-1	$[2Fe-2S]^{2+}$			
after cluster assembly	site 1	0.29	0.73	0.30
	site 2	0.29	0.50	0.30
	$[4Fe-4S]^{2+}$			
	pair 1	0.47	1.22	0.37
	pair 2	0.42	0.95	0.37
D37A NifU-1	$[2Fe-2S]^{2+}$			
after cluster assembly	site 1	0.28	0.68	0.30
	site 2	0.27	0.48	0.30
	$[4Fe-4S]^{2+}$			
	pair 1	0.47	1.29	0.29
	pair 2	0.45	1.00	0.32

[a] The estimated uncertainties for δ and ΔE_Q are 0.02 and 0.03 mm/s, respectively.

the assembled $[4Fe-4S]^{2+}$ cluster identified in samples of NifU repurified after NifS-mediated cluster assembly (cf. Tables 1 and 2). Quantification of the $[2Fe-2S]^{2+}$ and $[4Fe-4S]^{2+}$ components based on the NifU and ^{57}Fe concentrations in the reaction mixture (see the bottom of Figure 3) reveals that NifS-mediated assembly initially involves the assembly of 1 $[2Fe-2S]^{2+}$ cluster/NifU monomer in a process that is essentially complete after 45 min. At the same time, a $[4Fe-4S]^{2+}$ cluster is assembled at a slower rate, in a process that is close to completion after 90 min. Hence, after 90 min, NifU contains approximately 2 $[2Fe-2S]^{2+}$ clusters (1 assembled and 1 permanent cluster) and 1 assembled $[4Fe-4S]^{2+}$ cluster/monomer. After the reaction is allowed to continue for another 3 h, the stoichiometry of the assembled $[2Fe-2S]^{2+}$ clusters decreases to ~0.5/NifU monomer, while the stoichiometry of the assembled $[4Fe-4S]^{2+}$ clusters increases to ~1.5/NifU monomer, indicating a slow reductive conversion of 2 assembled $[2Fe-2S]^{2+}$ clusters to yield 1 $[4Fe-4S]^{2+}$ cluster. Considering the fact that slow conversion of 2 $[2Fe-2S]^{2+}$ to 1 $[4Fe-4S]^{2+}$ cluster has been observed in *Av* IscU during IscS-mediated cluster assembly (*40*) and that $[2Fe-2S]^{2+}$ clusters have been shown to assemble in the N-terminal (IscU-type) fragment of NifU (NifU-1) (*11*), it is suggested that the assembled $[2Fe-2S]^{2+}$ clusters are located in the N-terminal domain of NifU and can undergo slow reductive conversion to yield $[4Fe-4S]^{2+}$ clusters under the reaction conditions. If true, then the $[4Fe-4S]^{2+}$ clusters that form at the early stage of the assembly process must be assigned predominantly or exclusively to the C-terminal domain.

The observation that samples of NifU purified after NifS-mediated cluster assembly contain only 1 permanent $[2Fe-2S]^{2+}$ cluster and 1 assembled $[4Fe-4S]^{2+}$ cluster/NifU monomer indicates that all of the assembled $[2Fe-2S]^{2+}$ clusters and some of the assembled $[4Fe-4S]^{2+}$ clusters are lost during purification, suggesting different stabilities for clusters assembled onto different domains of NifU. To provide more definitive evidence for the type, location, and stability of clusters that can be assembled on NifU, NifS-

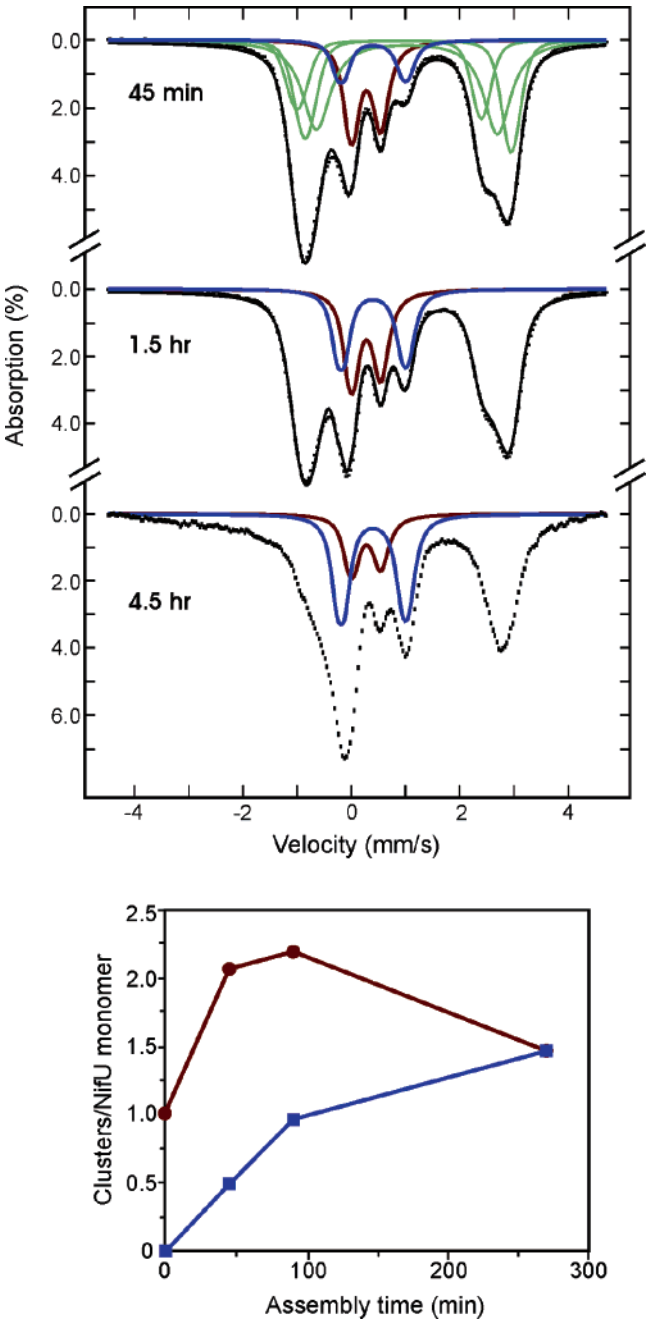

FIGURE 3: Time course of NifS-mediated cluster assembly on NifU monitored by Mössbauer spectroscopy. (Top) Mössbauer spectra of the reaction mixture at selected times during NifS-mediated cluster assembly on ^{57}Fe-enriched wild-type NifU using $^{57}Fe^{2+}$. Protein and reagent concentrations were as follows: 85 μM NifU, 2.4 μM NifS, 1.9 mM $^{57}Fe^{2+}$, and 8 mM L-cysteine. Spectra were recorded at 4.2 K with a magnetic field of 50 mT applied parallel to the γ radiation. Mononuclear high-spin Fe^{2+} species are shown in green; $[2Fe-2S]^{2+}$ clusters are shown in brown; $[4Fe-4S]^{2+}$ clusters are shown in blue; and composite simulations are shown in black. Parameters used in the simulations are listed in Table 2. (Bottom) Quantification of the $[2Fe-2S]^{2+}$ and $[4Fe-4S]^{2+}$ Mössbauer components based on the NifU and ^{57}Fe concentrations in the reaction mixture.

Table 2: Mössbauer Parameters for the Fe−S Clusters Detected in Samples of the Reaction Mixtures during NifS-Mediated Cluster Assembly on NifU Proteins with $^{57}Fe^{2+}$

NifU protein	cluster type	δ (mm/s)[a]	ΔE_Q (mm/s)[a]	line width (mm/s)
^{57}Fe-enriched	$[2Fe-2S]^{2+}$			
full-length NifU	site 1	0.29	0.62	0.31
	site 2	0.27	0.42	0.31
	$[4Fe-4S]^{2+}$			
	pair 1	0.46	1.21	0.30
	pair 2	0.40	1.10	0.30
natural abundance	$[2Fe-2S]^{2+}$			
NifU-2	site 1	0.27	0.59	0.27
	site 2	0.28	0.37	0.27
	$[4Fe-4S]^{2+}$			
	pair 1	0.47	1.29	0.29
	pair 2	0.45	1.00	0.32
NifU-1	$[2Fe-2S]^{2+}$			
	site 1	0.29	0.73	0.30
	site 2	0.29	0.50	0.30
	$[4Fe-4S]^{2+}$			
	pair 1	0.47	1.22	0.37
	pair2	0.42	0.95	0.37

[a] The estimated uncertainties for δ and ΔE_Q are 0.02 and 0.03 mm/s, respectively.

mediated cluster assembly studies were carried out using NifU fragments containing only the N- or C-terminal scaffolding domains.

NifS-Mediated Cluster Assembly on NifU-2. NifU-2 is a stable homodimeric protein containing only the central and C-terminal domains of full-length NifU (residue 126 to the C terminus, see Scheme 1) (*46*). Previous analytical and spectroscopic studies have confirmed the presence of a permanent $[2Fe-2S]^{2+,+}$ cluster in each monomer with electronic, magnetic, vibrational, and redox properties essentially indistinguishable from those of the permanent $[2Fe-2S]^{2+,+}$ cluster in wild-type full-length NifU (*46*). NifS-mediated cluster assembly studies were carried out using natural abundance Fe NifU-2 samples containing 0.85 permanent $[2Fe-2S]^{2+}$ clusters/monomer using a 8-fold excess of natural abundance Fe^{2+} for UV−vis absorption studies (see Figure 4) and a 15-fold excess of $^{57}Fe^{2+}$ for Mössbauer investigations (see Figure 5).[2] UV−vis absorption studies of the reaction mixture indicate the gradual appearance of a chromophore with a pronounced shoulder at ∼400 nm that is indicative of assembly of a $[4Fe-4S]^{2+}$ cluster over a period of 40 min (see Figure 4). This was confirmed and quantified by Mössbauer studies of the reaction mixture (see Figure 5), which indicate the gradual assembly of 1.0 $[4Fe-4S]^{2+}$ cluster/NifU-2 monomer over a period of 80 min. The parameters obtained for the $[4Fe-4S]^{2+}$ cluster are identical to those of the $[4Fe-4S]^{2+}$ cluster in full-length NifU samples purified after NifS-mediated cluster assembly (cf. Tables 1 and 2). In addition, the Mössbauer spectra reveal a quadrupole doublet with parameters that are indicative of the permanent $[2Fe-2S]^{2+}$ (cf. Tables 1 and 2) that accounts for 0.15−0.20 $[2Fe-2S]^{2+}$ clusters/NifU-2 monomer at all time points investigated. This component is attributed to a

[2] Mössbauer studies of NifS-mediated cluster assembly on ^{57}Fe-enriched, wild-type NifU using a 22-fold excess of natural abundance Fe^{2+} for 4.5 h did not reveal any significant loss of ^{57}Fe-enriched permanent $[2Fe-2S]^{2+}$ clusters. Hence, the permanent clusters on NifU do not undergo a significant Fe exchange during NifS-mediated cluster assembly.

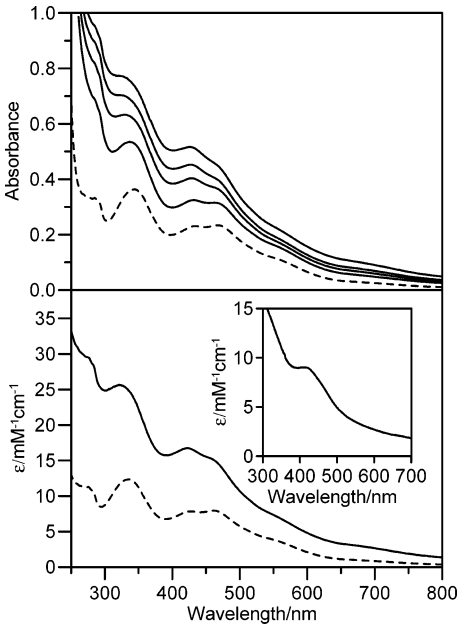

FIGURE 4: NifS-mediated assembly of Fe−S clusters on *A. vinelandii* NifU-2 monitored by UV−vis absorption. (Top) Time course of NifS-mediated cluster assembly on NifU-2. The dashed line is NifU-2 prior to the addition of NifS, cysteine, and Fe^{2+} ion, and the solid lines are spectra of the reaction mixture recorded at 10, 20, 30, and 40 min after initiating NifS-mediated cluster assembly (absorbance increasing with increasing time). Reaction mixture: 312 μM NifU-2, 7.8 μM NifS, 2.5 mM Fe^{2+}, and 10 mM L-cysteine. (Bottom) Purified NifU-2 before and after NifS-mediated cluster assembly. The dashed line is NifU-2 before NifS-mediated cluster assembly, and the solid line is NifU-2 after NifS-mediated cluster assembly for 2 h and repurification using Q-sepharose anion-exchange chromatography. The inset shows the difference spectrum corresponding to purified NifU-2 after minus before NifS-mediated cluster assembly.

rapid, NifS-mediated reconstitution of permanent $[2Fe-2S]^{2+}$ clusters on apo-NifU-2 (constitutes ∼15% of the total NifU-2 concentration). Hence, the Mössbauer studies of NifU-2 provide evidence for NifS-mediated assembly of 1 $[4Fe-4S]^{2+}$/monomer in the C-terminal domain of NifU. The absence of a transient $[2Fe-2S]^{2+}$ cluster during cluster assembly indicates that either the assembly of the C-terminal $[4Fe-4S]^{2+}$ cluster does not occur via $[2Fe-2S]^{2+}$ precursors or the conversion of $[2Fe-2S]^{2+}$ clusters to $[4Fe-4S]^{2+}$ clusters happens rapidly, preventing the transient $[2Fe-2S]^{2+}$ clusters to accumulate to a detectable level under the experimental conditions.

The $[4Fe-4S]^{2+}$ cluster assembled in the C-terminal domain of NifU-2 is largely or wholly retained during anaerobic purification as shown by Mössbauer, UV−vis absorption, and analytical studies of samples of NifU-2, repurified after NifS-mediated cluster assembly using an 8-fold excess of Fe^{2+}. Analytical data indicate 5.0 Fe atoms/NifU-2 monomer for these repurified samples. The Mössbauer spectrum of natural abundance Fe NifU-2 repurified after NifS-mediated cluster assembly for 90 min using ^{57}Fe (Figure 2C) shows that 83% of the ^{57}Fe absorption can be attributed to the C-terminal $[4Fe-4S]^{2+}$ cluster (shown in blue) and 9% to the permanent $[2Fe-2S]^{2+}$ cluster (shown in brown). Assuming that the repurified sample contains 1.7 natural abundance Fe atoms/monomer (85% occupancy of the permanent $[2Fe-2S]^{2+}$ clusters prior to NifS-mediated cluster assembly), the analytical data (5.0 Fe/monomer)

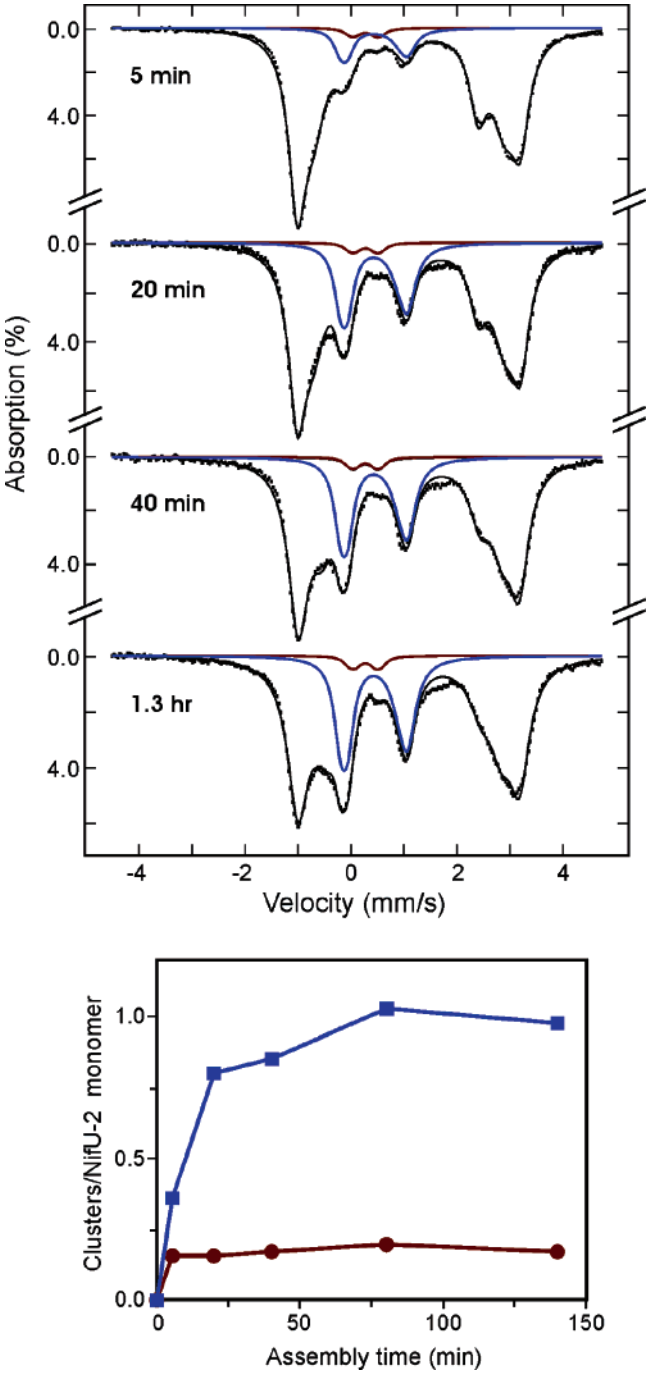

FIGURE 5: Time course of NifS-mediated cluster assembly on NifU-2 monitored by Mössbauer spectroscopy. (Top) Mössbauer spectra of the reaction mixture at selected times during NifS-mediated cluster assembly on natural abundance NifU-2 using $^{57}Fe^{2+}$. Protein and reagent concentrations were 160 μM NifU-2, 6 μM NifS, 2.4 mM $^{57}Fe^{2+}$, and 10 mM L-cysteine. Spectra were recorded at 4.2 K with a magnetic field of 50 mT applied parallel to the γ radiation. $[2Fe-2S]^{2+}$ clusters are shown in brown; $[4Fe-4S]^{2+}$ clusters are shown in blue; and composite simulations including Fe^{2+} species are shown in black. Parameters used in the simulations are listed in Table 2. (Bottom) Quantification of the $[2Fe-2S]^{2+}$ and $[4Fe-4S]^{2+}$ Mössbauer components based on the NifU-2 and ^{57}Fe concentrations in the reaction mixture.

together with the Mössbauer data indicate 0.7 $[4Fe-4S]^{2+}$ clusters/NifU-2 monomer and a complete reconstitution of all of the vacant permanent $[2Fe-2S]^{2+}$ sites with ^{57}Fe (see Table 1). The absorption spectra of purified samples after and before NifS-mediated cluster assembly are shown in the

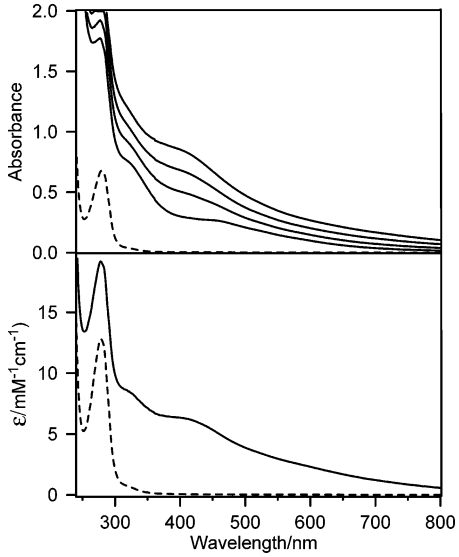

FIGURE 6: NifS-mediated assembly of Fe−S clusters on *A. vinelandii* NifU-1 monitored by UV−vis absorption. (Top) Time course of NifS-mediated cluster assembly on NifU-1. The dashed line is NifU-1 prior to addition of NifS, L-cysteine, and Fe^{2+} ion, and the solid lines are spectra of the reaction mixture recorded at 10, 20, 30, and 40 min after initiating NifS-mediated cluster assembly (absorbance increasing with increasing time). Reaction mixture: 530 μM NifU-1, 20 μM NifS, 4.8 mM Fe^{2+}, and 23 mM L-cysteine. (Bottom) Purified NifU-1 before and after NifS-mediated cluster assembly. The dashed line is NifU-1 before NifS-mediated cluster assembly, and the solid line is NifU-1 after NifS-mediated cluster assembly for 150 min and repurification using Q-sepharose anion-exchange chromatography.

bottom of Figure 4, and the difference absorption spectrum ($\epsilon_{400} = 9.6$ mM^{-1} cm^{-1}, see inset of Figure 4) is consistent with ~0.7 $[4Fe-4S]^{2+}$ clusters/monomer. The substoichiometric amounts of assembled $[4Fe-4S]^{2+}$ clusters in purified NifU-2 samples, as compared to the stoichiometric amounts of $[4Fe-4S]^{2+}$ clusters accumulated in the reaction mixture investigated by Mössbauer spectroscopy, are likely to reflect either minor cluster degradation during purification or the difference in excess of Fe^{2+} used in the cluster assembly reaction (8- and 15-fold, respectively). The fact that the $[4Fe-4S]^{2+}$ clusters assembled on NifU-2 are mostly retained after purification and that the Mössbauer parameters are identical to those of the $[4Fe-4S]^{2+}$ clusters found in full-length NifU repurified after cluster assembly suggests strongly that the $[4Fe-4S]^{2+}$ clusters in purified NifU reside in the C-terminal domain.

NifS-Mediated Cluster Assembly on Wild-Type NifU-1 and D37A NifU-1. NifU-1 is a stable homodimeric protein containing only the IscU-like N-terminal domain of full-length NifU (first 131 residues, see Scheme 1). Previous analytical, UV−vis absorption, and resonance Raman studies of wild-type NifU-1 demonstrated the assembly of substoichiometric amounts of labile $[2Fe-2S]^{2+}$ clusters (<0.3/NifU-1 monomer) in a NifS-mediated process (*11*). In the present work, the time course of NifS-mediated cluster assembly on NifU-1 has been reinvestigated by parallel UV−vis absorption and Mössbauer studies of a reaction mixture involving a 9-fold excess of $^{57}Fe^{2+}$ (see Figures 6 and 7), respectively. Absorption studies of the reaction mixture indicate initial formation of a chromophore with a shoulder centered near 450 nm after 10 min and a progressive blue shift to yield a chromophore with a shoulder centered at 400

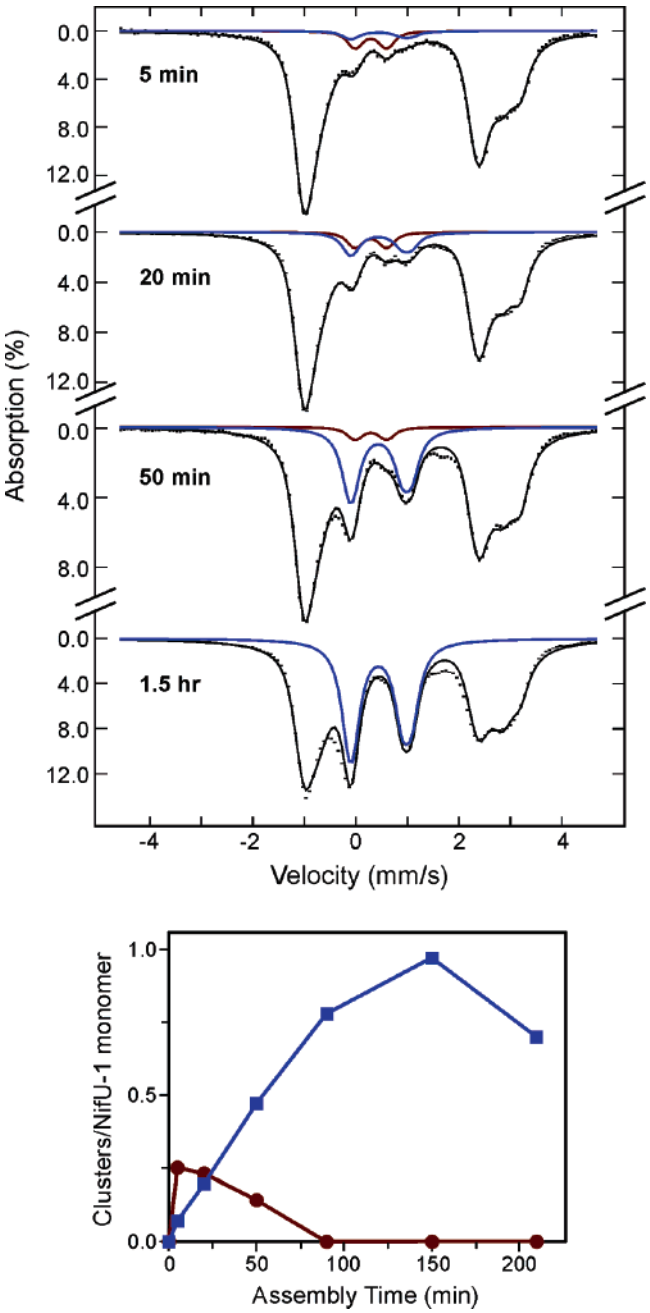

FIGURE 7: Time course of NifS-mediated cluster assembly on NifU-1 monitored by Mössbauer spectroscopy. (Top) Mössbauer spectra of the reaction mixture at selected times during NifS-mediated cluster assembly on NifU-1 using $^{57}Fe^{2+}$. Protein and reagent concentrations were 530 μM NifU-1, 20 μM NifS, 4.8 mM $^{57}Fe^{2+}$, and 23 mM L-cysteine. Spectra were recorded at 4.2 K with a magnetic field of 50 mT applied parallel to the γ radiation. $[2Fe-2S]^{2+}$ clusters are shown in brown; $[4Fe-4S]^{2+}$ clusters are shown in blue; and composite simulations including Fe^{2+} species are shown in black. Parameters used in the simulations are listed in Table 2. (Bottom) Quantification of the $[2Fe-2S]^{2+}$ and $[4Fe-4S]^{2+}$ Mössbauer components based on the NifU-1 and ^{57}Fe concentrations in the reaction mixture.

nm after 40 min. Such absorption behavior is consistent with sequential formation of $[2Fe-2S]^{2+}$ and $[4Fe-4S]^{2+}$ clusters, and this interpretation is supported by the Mössbauer studies of the reaction mixture shown in Figure 7. Mössbauer studies demonstrate that the initial products of NifS-mediated cluster assembly on NifU-1 are $[2Fe-2S]^{2+}$ clusters with quadrupole splittings and isomer shifts that are distinct from those established for the permanent $[2Fe-2S]^{2+}$ cluster on NifU (see Table 2). Quantification of the Mössbauer absorption based on the protein and ^{57}Fe concentrations (9 Fe atoms/NifU-1 monomer) indicates a rapid accumulation of 0.25 $[2Fe-2S]^{2+}$ clusters/NifU-1 monomer during the first 5 min of NifS-mediated cluster assembly. The $[2Fe-2S]^{2+}$/NifU-1 ratio then gradually decreases to 0 over the next 85 min, with a concomitant increase in the $[4Fe-4S]^{2+}$/NifU-1 ratio. The assembled $[4Fe-4S]^{2+}$ clusters have Mössbauer parameters that are distinct from (though similar to) those established for the $[4Fe-4S]^{2+}$ clusters assembled in the C-terminal domain of NifU and NifU-2 (see Table 2) and reach a maximum concentration of 0.97 $[4Fe-4S]^{2+}$ clusters/NifU-1 monomer after 150 min. The $[4Fe-4S]^{2+}$ cluster concentration eventually starts to decrease at longer times. The Mössbauer spectrum of a NifU-1 sample purified after NifS-mediated cluster assembly for ~40 min (Figure 2D) shows the presence of both assembled clusters. Quantification of the Mössbauer resonances based on Fe and protein analyses indicates 0.2 $[4Fe-4S]^{2+}$ clusters and 0.1 $[2Fe-2S]^{2+}$ clusters/NifU-1 monomer for this purified sample.[3] These cluster stoichiometries are lower than expected at this time point during the assembly process and suggest partial degradation of the assembled clusters during purification.

When the Mössbauer time course studies of NifU-1 are taken at face value, they would appear to suggest that 1 $[4Fe-4S]^{2+}$ cluster can be assembled in the N-terminal domain of each NifU monomer. However, characterization of samples of NifU-1 repurified after NifS-mediated cluster assembly has always yielded <0.5 $[4Fe-4S]^{2+}$ clusters/NifU-1 monomer. The absorption spectra are characteristic of $[4Fe-4S]^{2+}$ clusters but maximally have $\epsilon_{400} = 7$ mM^{-1} cm^{-1}, indicating <0.5 $[4Fe-4S]^{2+}$ cluster/monomer (extinction coefficients for $[4Fe-4S]^{2+}$ centers at 400 nm are typically 15−16 mM^{-1} cm^{-1}) (see the bottom of Figure 6). Also, a previous Mössbauer investigation of similar reaction mixtures excluding the scaffolding proteins (*18*) indicates that spontaneous self-assembly of $[4Fe-4S]^{2+}$ clusters in aqueous solution is possible, presumably with cysteinate terminal ligation, even though these clusters are minor components that never exceed 10% of the total Fe present in the solution. Thus, it is possible that the assembled $[4Fe-4S]^{2+}$ clusters are not all protein-bound. In other words, it is likely that NifU-1 as well as the N-terminal domain of NifU provide a scaffold for efficient assembly of labile $[4Fe-4S]^{2+}$ clusters, via $[2Fe-2S]^{2+}$ cluster intermediates, that can be exported intact into the medium (23 mM in L-cysteine) to yield cysteinate-ligated $[4Fe-4S]^{2+}$ clusters that are free in aqueous solution.

Previous analytical, UV−vis absorption, and resonance Raman studies of NifU-1 indicated that the D37A mutation stabilizes assembled $[2Fe-2S]^{2+}$ clusters (*11*), and a similar result was subsequently reported for the equivalent mutation in human IscU (*43*). Consequently NifS-mediated cluster assembly studies monitored by Mössbauer spectroscopy were carried out on D37A NifU-1 to determine if this substitution prevents the assembly of $[4Fe-4S]^{2+}$ clusters. UV−vis

[3] A portion of the broad and ill-defined underlying absorption observed in the spectrum of Figure 2D may be attributable to a $[4Fe-4S]^{+}$ cluster that accounts for approximately 0.05 cluster/NifU-1 monomer. However, a definitive assignment cannot be made because of the weak absorption intensity and overlapping contributions from other Fe species.

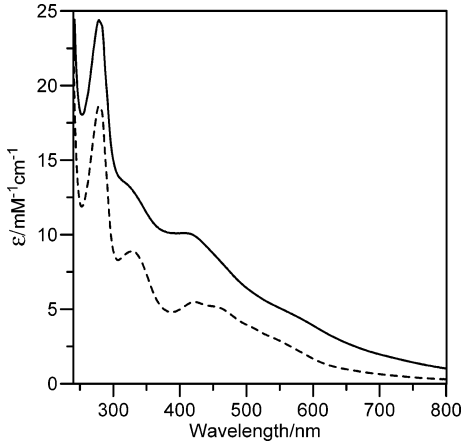

FIGURE 8: UV−vis absorption spectra of *A. vinelandii* D37A NifU-1 repurified after 20 min (- - -) and 50 min (—) of NifS-mediated cluster assembly. Cluster assembly conditions: 500 μM NifU-1, 20 μM NifS, 4.5 mM Fe^{2+}, and 23 mM L-cysteine in 100 mM Tris/HCl buffer at pH 7.8, with 0.1 M NaCl.

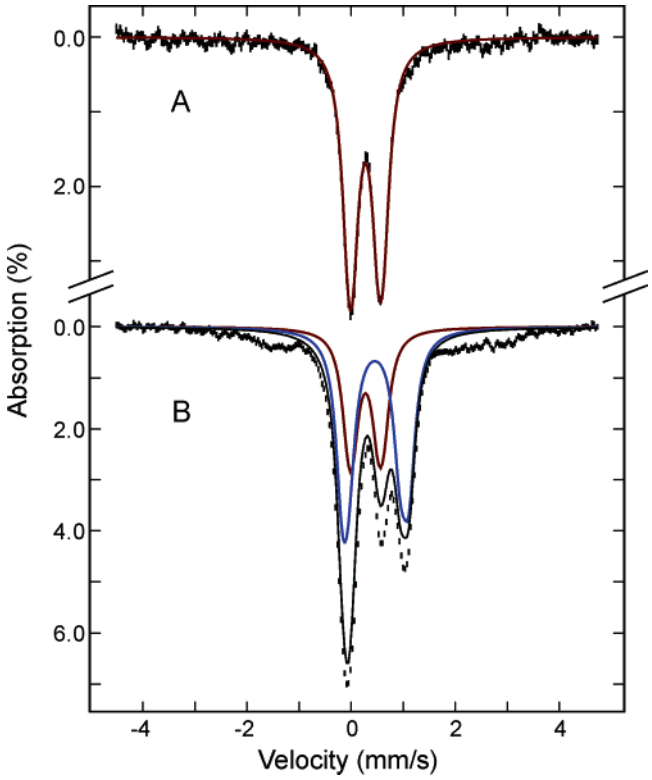

FIGURE 9: Mössbauer spectra of *A. vinelandii* D37A NifU-1 repurified after 20 min (A) and 50 min (B) of NifS-mediated cluster assembly using $^{57}Fe^{2+}$. The cluster assembly conditions are described in Figure 8. Spectra were recorded at 4.2 K with a magnetic field of 50 mT applied parallel to the γ radiation. $[2Fe-2S]^{2+}$ clusters are shown in brown; $[4Fe-4S]^{2+}$ clusters are shown in blue; and composite simulations are shown in black. Parameters used in the simulations are listed in Table 1.

absorption and Mössbauer spectra of samples of D37A NifU-1 repurified after 20 and 50 min of NifS-mediated cluster assembly using an 8-fold excess of $^{57}Fe^{2+}$ are shown in Figures 8 and 9, respectively. In accordance with previous results (*11*), both Mössbauer and absorption spectra indicate that the sample repurified after 20 min of NifS-mediated cluster assembly contains only $[2Fe-2S]^{2+}$ clusters and that Fe and protein determinations indicate 0.5 $[2Fe-2S]^{2+}$ clusters/NifU-1 monomer. However, both the Mössbauer and absorption spectra show that samples repurified after 50 min of NifS-mediated cluster assembly contain a mixture of $[2Fe-2S]^{2+}$ and $[4Fe-4S]^{2+}$ clusters. In the absorption spectrum, the presence of $[4Fe-4S]^{2+}$ clusters is evident by the emergence of a pronounced shoulder at 400 nm and a partial loss of the absorption at 330 nm. In the Mössbauer spectrum (Figure 9B), quadrupole doublets that are indicative of $[2Fe-2S]^{2+}$ clusters (shown in brown) and $[4Fe-4S]^{2+}$ clusters (shown in blue) account for 80% of the Fe in the sample, with the remaining Fe exhibiting a broad and ill-defined underlying absorption typical of polymeric iron sulfides. On the basis of Fe and protein determinations, the sample contains 0.25 $[2Fe-2S]^{2+}$ and 0.2 $[4Fe-4S]^{2+}$ clusters/NifU-1 monomer. The observed decrease in the $[2Fe-2S]^{2+}$ cluster stoichiometry and increase in the $[4Fe-4S]^{2+}$ cluster stoichiometry with time are again consistent with reductive coupling of 2 $[2Fe-2S]^{2+}$ clusters to yield 1 $[4Fe-4S]^{2+}$ cluster/NifU-1 dimer. Although these results clearly demonstrate that D37 is not required for $[4Fe-4S]^{2+}$ cluster formation in the N-terminal domain of NifU, the difference in the Mössbauer parameters for the $[4Fe-4S]^{2+}$ clusters in purified samples of wild-type NifU-1 and D37A NifU-1 (see Table 1) indicates that D37 does affect the properties of the assembled $[4Fe-4S]^{2+}$ cluster. As discussed below, this effect is also manifest in the ability to transfer the assembled $[4Fe-4S]^{2+}$ cluster to an acceptor protein.

Cluster Transfer from NifU to Apo-Fe Protein. Purified samples of NifU, NifU-2, NifU-1, and D37A NifU-1 with spectroscopically and analytically defined cluster contents were incubated with apo-Fe protein in a 2:1 ratio (2 mol of dimeric NifU/1 mol of dimeric Fe protein) to assess if clusters assembled in the N- and C-terminal domain of NifU can be used to rapidly assemble subunit-bridging $[4Fe-4S]^{2+}$ clusters on the apo form of the homodimeric Fe protein. Restoration of the [4Fe−4S] cluster on apo-Fe protein was monitored by a coupled assay in which nitrogenase hydrogen production is monitored as previously described (*47*) (see Figure 10). Samples were assayed immediately after mixing NifU samples with apo-Fe protein samples (<5 min). The same results were obtained when assays were performed 30 min after mixing NifU samples with apo-Fe protein samples, indicating that cluster transfer from NifU to the apo-Fe protein is complete prior to the assay. Fe-protein activity is represented as a percentage of the activity of holo-Fe protein in the nitrogenase hydrogen-evolution assay (800 nmol H_2/mg of Fe protein). The results indicate that samples of NifU and NifU-2 containing, respectively, 0.8 and 0.7 $[4Fe-4S]^{2+}$ clusters/monomer, predominantly or exclusively in the C-terminal domain, are both very effective in reactivating apo-Fe protein, 93 and 90%, respectively. A lower level of apo-Fe protein reactivation, 35%, was observed with NifU-1, containing 0.2 $[4Fe-4S]^{2+}$ and 0.1 $[2Fe-2S]^{2+}$ clusters/monomer as judged by analytical and Mössbauer studies, but the titration results discussed below suggest that this reflects the low assembled cluster content of the NifU-1 sample. Parallel studies in which NifU samples were replaced in the assay with a 20-fold molar excess of Fe^{2+} and S^{2-}/apo-Fe-protein dimer, afforded only 10% activation of the apo-Fe protein. This control experiment demonstrates that $[4Fe-4S]^{2+}$ clusters assembled on the N-terminal (NifU-1) or C-terminal (NifU and NifU-2) domains of NifU are transferred intact to apo-Fe protein, rather than being

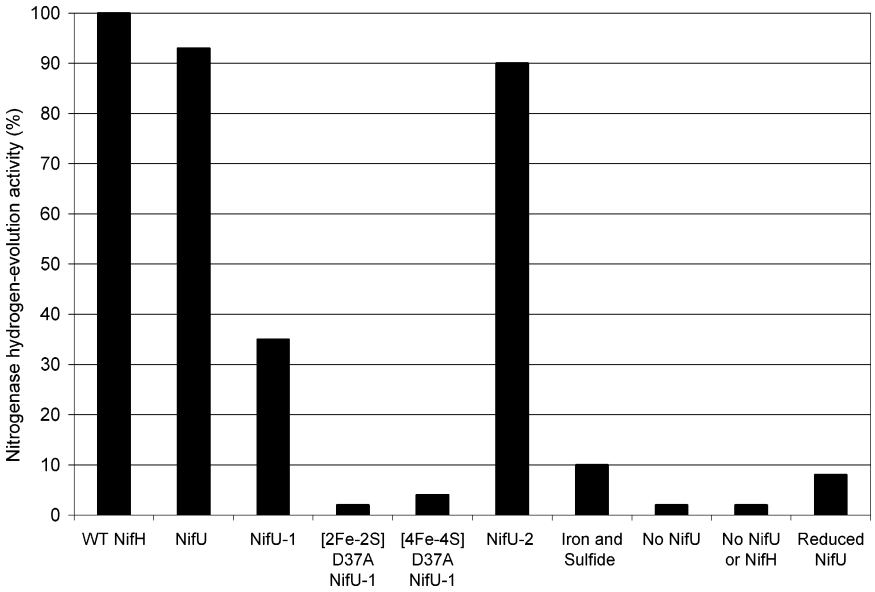

FIGURE 10: Comparison of the ability of NifU samples with spectroscopically defined Fe−S cluster compositions to assemble a [4Fe−4S] cluster on nitrogenase apo-Fe protein as assessed by the nitrogenase hydrogen evolution assay described in the Materials and Methods. For all samples involving NifU, the molar ratio of dimeric NifU/dimeric apo-Fe protein was 2:1. NifU = wild-type NifU containing 0.9 $[2Fe-2S]^{2+}$ (permanent) cluster and 0.8 $[4Fe-4S]^{2+}$ cluster/monomer and apo-Fe protein; NifU-1 = NifU-1 containing 0.2 $[4Fe-4S]^{2+}$ and 0.1 $[2Fe-2S]^{2+}$ clusters/monomer and apo-Fe protein; [2Fe−2S] D37A NifU-1 = D37A NifU-1 containing 0.50 $[2Fe-2S]^{2+}$ cluster/monomer and apo-Fe protein; [4Fe−4S] D37A NifU-1 = D37A NifU-1 containing 0.25 $[2Fe-2S]^{2+}$ and 0.2 $[4Fe-4S]^{2+}$ clusters/monomer and apo-Fe protein; NifU-2 = NifU-2 containing 1.0 $[2Fe-2S]^{2+}$ (permanent) cluster and 0.70 $[4Fe-4S]^{2+}$ cluster/monomer and apo-Fe protein; iron and sulfide = apo-Fe protein plus a 20-fold excess of Fe^{2+} and S^{2-}; no NifU = apo-Fe protein without NifU; no NifU or NifH = no NifU and apo-Fe protein in assay mixture; and reduced NifU = wild-type NifU containing 0.9 $[2Fe-2S]^{2+}$ (permanent) cluster and 0.8 $[4Fe-4S]^{2+}$ cluster/monomer incubated with a 10-fold excess of dithionite for 30 min before incubation with apo-Fe protein.

degraded and then reassembled on apo-Fe protein. This conclusion was further substantiated by apo-Fe protein activation studies involving dithionite-reduced NifU. When NifU containing approximately 1 permanent $[2Fe-2S]^{2+,+}$ and 1 assembled $[4Fe-4S]^{2+}$ cluster/monomer was incubated with dithionite for 30 min prior to mixing with apo-Fe protein, only 8% apo-Fe protein reactivation was detected. Because the combination of Mössbauer, EPR, and UV−vis absorption studies have shown that $[4Fe-4S]^{2+}$ clusters assembled in the C-terminal domain of NifU and NifU-2 are degraded upon reduction with excess dithionite, the failure to activate apo-Fe protein by the dithionite-reduced NifU, which prior to dithionite reduction was able to fully activate apo-Fe proteins, also argues strongly for intact $[4Fe-4S]^{2+}$ cluster transfer from NifU to the apo-Fe protein.

Two cluster-bound forms of D37A NifU-1 containing 0.50 $[2Fe-2S]^{2+}$ clusters/monomer and 0.25 $[2Fe-2S]^{2+}$ and 0.2 $[4Fe-4S]^{2+}$ clusters/monomer, respectively, were also tested for their ability to activate apo-Fe protein (see Figure 10). Neither sample was effective in activating apo-Fe protein as judged by levels of activation, 2 and 4%, respectively, that are similar to the basal levels of nitrogenase hydrogen-evolution activity in the absence of NifU or NifU and apo-Fe protein. Furthermore, increasing the molar ratio of D37A NifU-1/apo-Fe protein from 2:1 to 8:1 did not result in significantly enhanced levels of activation, 3 and 7%, respectively (data not shown). These results clearly implicate a role for D37 in transferring clusters assembled in the N-terminal domain of NifU to the apo-Fe protein.

The stoichiometry of apo-Fe protein activation by NifU, NifU-2, and NifU-1 samples with preassembled clusters was assessed by activation studies as a function of the NifU/apo-Fe protein molar ratio (see Figure 11). The titration curves

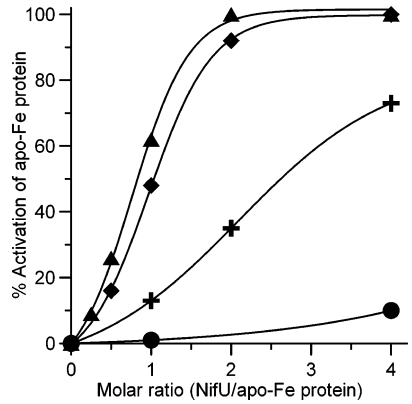

FIGURE 11: Titration of [4Fe−4S] cluster assembly on nitrogenase apo-Fe protein as a function of the increasing concentration of NifU samples with spectroscopically defined Fe−S cluster compositions: wild-type NifU containing 0.9 $[2Fe-2S]^{2+}$ (permanent) cluster and 0.8 $[4Fe-4S]^{2+}$ cluster/monomer (▲); NifU-2 containing 1.0 $[2Fe-2S]^{2+}$ (permanent) cluster and 0.70 $[4Fe-4S]^{2+}$ cluster/monomer (◆); NifU-1 containing 0.2 $[4Fe-4S]^{2+}$ and 0.1 $[2Fe-2S]^{2+}$ clusters/monomer (+); control without NifU and with addition of $4Fe^{2+}$ and $4S^{2-}$/apo-Fe protein dimer corresponding to a molar ratio of 1.0 (●). Molar ratio corresponds to dimeric NifU/dimeric Fe protein. [4Fe−4S] cluster assembly was monitored via Fe-protein activity as measured by the nitrogenase hydrogen evolution assay as described in the Materials and Methods.

scale according to the assembled $[4Fe-4S]^{2+}$ cluster content of the samples (0.8, 0.7, and 0.2/monomer, respectively). According to the titration curves of NifU and NifU-2, which contains only $[4Fe-4S]^{2+}$ as the assembled cluster, a 4-fold excess of transient $[4Fe-4S]^{2+}$ clusters (i.e., 2:1 ratio of dimeric NifU/dimeric apo-Fe protein) is required to effect complete activation of apo-Fe protein. The fact that NifU-1 contains a mixture of assembled $[4Fe-4S]^{2+}$ and $[2Fe-2S]^{2+}$

clusters complicates interpretation of this activation study and raises the question of whether the observed activation involves the transfer of the assembled $[2Fe-2S]^{2+}$ clusters. However, even if 100% efficient $[2Fe-2S]^{2+}$ cluster transfer is assumed, the observed high level of activation by NifU-1 (>70% at a 4:1 NifU-1/apo-Fe protein ratio) cannot be achieved by transferring solely the low level of $[2Fe-2S]^{2+}$ clusters contained in NifU-1 (0.1 cluster/NifU-1 monomer). Thus, activation of apo-Fe protein by NifU-1 must involve the transfer of the assembled $[4Fe-4S]^{2+}$ clusters, although activation by the transfer of $[2Fe-2S]^{2+}$ clusters cannot be excluded. Hence, on the basis of cluster stoichiometry, both the C- and N-terminal $[4Fe-4S]^{2+}$ clusters preassembled on NifU or NifU fragments appear to be equally effective in activating apo-Fe protein.

DISCUSSION

Genetic and biochemical studies have demonstrated a crucial role for NifU in nitrogen-fixation-specific Fe−S cluster assembly (*4*), and recent studies also implicate the involvement of NifU-like proteins in general Fe−S cluster biosynthesis in some non-nitrogen-fixing bacteria and eukaryotic organisms (*19*, *20*). Although previous spectroscopic studies implicated a role for the N-terminal domain of NifU as a scaffold of NifS-mediated cluster assembly (*11*), NifU is a modular protein comprising three distinct domains (*46*) (see Scheme 1) and hence is considerably more complex than the U- and A-, and Nfu-type Fe−S cluster scaffolding proteins that are used in general Fe−S cluster biosynthesis (*4*). Moreover, recent genetic and biochemical studies of NifU indicated that both the N- and C-terminal domains are functional in mediating assembly of the [4Fe−4S] cluster on apo nitrogenase Fe protein (*47*). Hence, the objective of the research described herein was to characterize the roles of the IscU-type N-terminal domain and Nfu-type C-terminal domain of NifU via *in vitro* analytical and spectroscopic studies of NifS-mediated cluster assembly on NifU and NifU fragments. The results demonstrate that both the N- and C-terminal domains of NifU provide scaffolds for the assembly of Fe−S clusters that can be used for the maturation of the apo form of the nitrogenase Fe protein. Moreover, they provide a good indication of the type, stoichiometry, and stability of the clusters that can be assembled in each scaffolding domain of NifU and the first well-documented example of transfer of a $[4Fe-4S]^{2+}$ cluster from a scaffold protein to an acceptor apoprotein. Our proposed model for the time course of cluster assembly on full-length NifU is shown in Figure 12, and the cluster assembly processes on the C- and N-terminal domains are discussed separately below.

Nfu and CnfU proteins with homology to the C-terminal domain of NifU have been characterized in cyanobacteria, plants, and higher organisms and shown to have a role in Fe−S cluster biosynthesis (*12*, *44*, *45*, *55*, *56*). In plants and cyanobacteria, UV−vis absorption studies indicate that these proteins bind $[2Fe-2S]^{2+}$ clusters that can be transferred *in vitro* to apo-ferredoxin (*12*, *44*). However, the cluster type and stoichiometry have yet to be established on the basis of analytical and Mössbauer data. In contrast, analytical, UV−vis absorption and Mössbauer studies of human Nfu have demonstrated the ability to assemble a $[4Fe-4S]^{2+}$ cluster (approximately 1 $[4Fe-4S]^{2+}$ cluster/2 Nfu monomers in

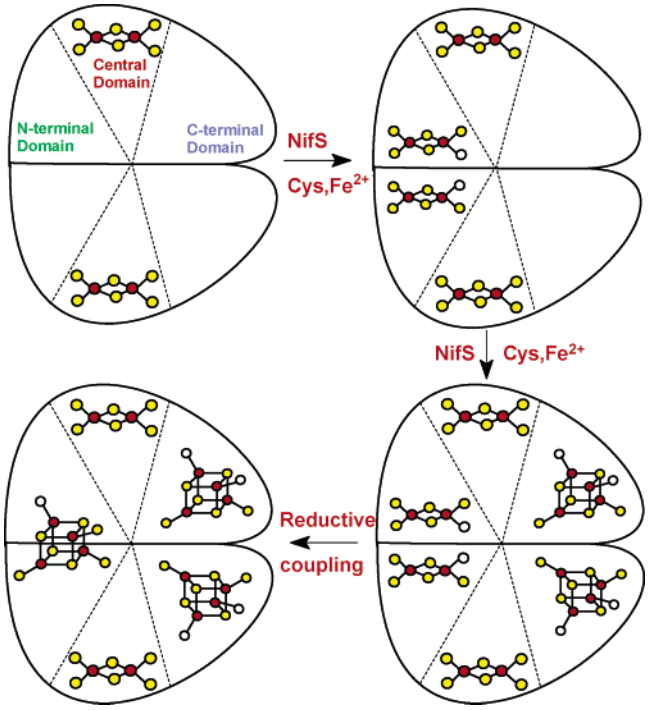

FIGURE 12: Proposed model for the time course of NifS-mediated cluster assembly on NifU. The location of the C-terminal $[4Fe-4S]^{2+}$ clusters, i.e., each within a subunit or both bridging subunits, has yet to be determined. Red = Fe; yellow = S; and white = noncysteinyl ligand.

purified samples) (*45*). The NifS-mediated cluster assembly studies involving full-length NifU and NifU-2 reported in this work indicate that the C-terminal domain of NifU can assemble 1 $[4Fe-4S]^{2+}$ cluster/monomer and that these clusters are largely retained during purification. This is demonstrated by the ability to purify samples of NifU-2 with 0.7 $[4Fe-4S]^{2+}$ clusters/monomer, coupled with the observation that the time course of NifS-mediated cluster assembly on NifU-2 asymptotically approaches 1.0 $[4Fe-4S]^{2+}$/monomer assembly (see Figure 5). In addition, identical Mössbauer parameters are obtained for the $[4Fe-4S]^{2+}$ clusters in samples of NifU and NifU-2 purified after cluster assembly. When these observations are taken together, they argue strongly for 1 $[4Fe-4S]^{2+}$ cluster/monomer and for the conclusion that stoichiometric $[4Fe-4S]^{2+}$ clusters present in purified samples of full-length NifU after NifS-mediated cluster assembly are predominantly or exclusively in the C-terminal domain. Mutagenesis and/or structural studies will be required to identify the location and ligation of these clusters, with the two conserved cysteines in the CXXC motif (Cys272 and Cys275 in *Av* NifU) and the two conserved aspartates in the DXXD motif (Asp250 and Asp253 in *Av* NifU), representing the most likely candidates for cluster ligands.

Mössbauer studies of the time course of NifS-mediated cluster assembly on NifU and NifU-2 also provide insight into the mechanism of $[4Fe-4S]^{2+}$ assembly on the C-terminal domain. In contrast to the N-terminal domain, cluster assembly studies involving NifU-2 indicate that $[4Fe-4S]^{2+}$ cluster assembly in the C-terminal domain does not proceed via a stable $[2Fe-2S]^{2+}$ cluster intermediate. In addition, a comparison of the time course of cluster assembly on NifU and NifU-2 indicates that the initial $[4Fe-4S]^{2+}$ cluster assembly occurs at approximately the same rate, irrespective

of the presence of the N-terminal domain. This observation is consistent with the proposal that the $[4Fe-4S]^{2+}$ clusters assembled on NifU at the early stage of cluster assembly are located at the C-terminal domain and argue against the possibility that the $[4Fe-4S]^{2+}$ clusters are assembled in the N-terminal domain and then transferred to the C-terminal domain. Such considerations provide the basis of the proposed model for the time course of cluster assembly in the C-terminal domain of full-length NifU (see Figure 12).

NifS-mediated cluster assembly studies with NifU and NifU-1 provide several new insights into cluster assembly on the N-terminal domain of NifU, in particular, and on U-type scaffold proteins, in general. The time course of cluster assembly on NifU shows that, in addition to the permanent $[2Fe-2S]^{2+}$ cluster, a transient $[2Fe-2S]^{2+}$ cluster is assembled concomitantly with the assembly of the initial $[4Fe-4S]^{2+}$ cluster (see Figure 3). Because the initial $[4Fe-4S]^{2+}$ cluster assembly appears to occur in the C-terminal domain (as discussed above), the transient $[2Fe-2S]^{2+}$ cluster is most likely assembled on the N-terminal domain. Evidence supporting this assessment is provided by the time course of cluster assembly on NifU-1, which also shows the accumulation of a transient $[2Fe-2S]^{2+}$ cluster that precedes the assembly of $[4Fe-4S]^{2+}$ clusters (see Figure 7). However, while the transient $[2Fe-2S]^{2+}$ cluster in NifU-1 accumulates to only a substoichiometric amount of <0.3 cluster/NifU-1 monomer, the presence of the C-terminal domain in NifU appears to have affected the stability of the transient $[2Fe-2S]^{2+}$ cluster, allowing it to build up to a stoichiometric quantity of 1 cluster/NifU monomer. Such considerations lead to the conclusion that the time course of cluster assembly on the N-terminal domain of full-length NifU closely mimics that previously characterized with *Av* IscU (*40*). The process initially involves rapid assembly of $[2Fe-2S]^{2+}$ clusters, reaching a maximum content of 1 in each monomeric NifU. Over time, the accumulation of $[2Fe-2S]^{2+}$ clusters decreases with concomitant increase in $[4Fe-4S]^{2+}$ clusters, suggesting reductive coupling of 2 $[2Fe-2S]^{2+}$ clusters to yield 1 $[4Fe-4S]^{2+}$ cluster formed at the subunit interface (see Figure 12).

Both the $[2Fe-2S]^{2+}$ and $[4Fe-4S]^{2+}$ clusters assembled on the N-terminal domain of full-length NifU are labile and do not appear to be present in samples of NifU purified after NifS cluster assembly, suggesting that either type of cluster has the capability to be transferred to acceptor apoproteins. In other words, it is possible that assembly of $[4Fe-4S]^{2+}$ clusters on apo acceptor proteins using U-type scaffolds could involve either transfer of preassembled labile $[4Fe-4S]^{2+}$ clusters, as demonstrated in this work, or sequential transfer of 2 preassembled $[2Fe-2S]^{2+}$ clusters that are reductively coupled on the acceptor protein, as suggested by the activation of apo adenosine 5′-phosphosulfate reductase using [2Fe−2S]-containing IscA (*16*). Thus far, the assembly of $[4Fe-4S]^{2+}$ clusters on U-type domains or proteins has only been demonstrated for *Av* IscU (*40*) and the N-terminal domain of *Av* NifU (this paper). While we cannot exclude the possibility that some U-type scaffold proteins, such as the IscU or Isu proteins from *E. coli* (*41*), *S. pombe* (*42*), and *Homo sapiens* (*14*, *43*) and SufU from *T. maritima* (*34*), are specific for assembly and transfer of $[2Fe-2S]^{2+}$ clusters only, the lability of the $[4Fe-4S]^{2+}$ clusters assembled on the N-terminal domain of NifU offers an attractive alternative explanation, namely, that $[4Fe-4S]^{2+}$ clusters are assembled and rapidly exported but are too labile to be purified intact on the U-type scaffold proteins. Mössbauer studies of the time course of cluster assembly on a wider variety of U-type scaffold proteins will be required to address this question.

Cluster transfer experiments involving NifU, NifU2, and NifU-1 samples with spectroscopically and analytically defined cluster composition and apo-Fe protein have provided the first well-documented examples of transfer of a $[4Fe-4S]^{2+}$ cluster from a scaffold protein to an acceptor protein. The assembly of $[4Fe-4S]^{2+}$ clusters on acceptor proteins using scaffold proteins with preformed clusters had previously been demonstrated only with mixed [2Fe−2S] and [4Fe−4S] cluster-containing forms of SufA and IscA and apo biotin synthase (*33*, *57*) and with [2Fe−2S]-containing IscA and apo adenosine 5′-phosphosulfate reductase (*16*). Moreover, transfer of $[4Fe-4S]^{2+}$ clusters from both the C- and N-terminal domains of NifU to apo-Fe protein occurs at least an order of magnitude faster and with equal or better efficiency than any published example of *in vitro* cluster transfer from a U-, A-, or Nfu-type scaffold protein to an acceptor protein, using the equivalent acceptor/donor protein stoichiometry (*12*−*16*, *33*, *34*, *42*, *44*, *57*). The rate and efficiency of $[4Fe-4S]^{2+}$ cluster transfer for the N- and C-terminal domains of NifU to apo-Fe protein are similar on a per cluster basis, and both are essentially complete within 5 min of mixing the proteins. Hence, $[4Fe-4S]^{2+}$ cluster transfer from NifU to an appropriate acceptor protein occurs at rates approaching physiologically relevant rates and does not appear to require any additional accessory proteins.

In accordance with previous results for NifU-1 (*11*) and IscU/Iscu or SufU proteins in *S. pombe*, *E. coli*, and *T. maritima* (*14*, *34*, *42*, *43*), the D37A variant was found to stabilize $[2Fe-2S]^{2+}$ clusters assembled in U-type scaffolding domains. The current study also demonstrates that the D37A variant does not significantly impede reductive coupling of 2 $[2Fe-2S]^{2+}$ clusters to yield 1 $[4Fe-4S]^{2+}$ cluster in NifU-1. However, the presence of D37 does affect the properties of both $[4Fe-4S]^{2+}$ and $[2Fe-2S]^{2+}$ clusters assembled on NifU-1. This is evident by the differences in the Mössbauer parameters for both the $[4Fe-4S]^{2+}$ and $[2Fe-2S]^{2+}$ clusters in purified samples of wild-type and D37A NifU-1 (see Table 1) and the resonance Raman spectra of the $[2Fe-2S]^{2+}$ clusters in wild-type and D37A NifU-1 (*58*). The structural origin of these spectroscopic differences are not known at present, but they could be interpreted in terms of D37, providing a cluster ligand and/or controlling cluster solvent exposure, in light of the proximity of D37 to the three conserved cysteine residues in the solvent-exposed cluster-binding site (*30*). The latter possibility seems very plausible, because the D37A substitution dramatically inhibits transfer of clusters assembled on NifU-1 to apo-Fe protein. A 10-fold decrease in the rate of transfer of $[2Fe-2S]^{2+}$ clusters from human and *S. pombe* Isu to apo ferredoxin was found to accompany the equivalent mutation in human and *S. pombe* Isu and interpreted in terms of a key role for this conserved aspartate in mediating cluster transfer by maintaining a solvent-exposed and accessible cluster on IscU (*14*).

Finally, we turn to the question of why NifU has two functional scaffolding domains: an N-terminal domain that has the capability to assemble and transfer both $[2Fe-2S]^{2+}$ and $[4Fe-4S]^{2+}$ clusters and a C-terminal domain that can

assemble and transfer $[4Fe-4S]^{2+}$ clusters. Clearly, NifU provides a versatile scaffold for assembly of $[2Fe-2S]^{2+}$ and $[4Fe-4S]^{2+}$ clusters, and this likely accounts for NifU being the only type of scaffold protein that is known to be present in *Helicobacter pylori* (*19*) and *Entamoeba histolytica* (*20*). Previous *in vivo* studies indicate redundant functions for the N- and C-terminal domains under diazotrophic growth conditions (*47*). However, the absence of a phenotype for substitutions involving either of the two C-terminal cysteines (*46*) indicates that the N-terminal domain has the dominant role in nitrogenase-specific Fe−S cluster assembly. It is tempting to speculate that NifU evolved as a scaffold protein with two separate domains each capable of rapid delivery of $[4Fe-4S]^{2+}$ clusters, to facilitate optimal assembly of fused double-cubane clusters such as the nitrogenase P cluster. Alternatively, each NifU scaffolding domain may be optimized for the assembly of Fe−S centers on distinct *nif*-specific proteins or to operate under distinct metabolic conditions. Future studies are planned to address the role of the two Fe−S cluster scaffolding domains on NifU.

REFERENCES

1. Beinert, H., Holm, R. H., and Münck, E. (1997) Iron−sulfur clusters; Nature's modular, multipurpose structures, *Science 277*, 653−659.
2. Johnson, M. K., and Smith, A. D. (2005) Iron−sulfur proteins, in *Encyclopedia of Inorganic Chemistry* (King, R. B., Ed.) 2nd ed., John Wiley and Sons, Chichester, U.K., in press.
3. Mansy, S. S., and Cowan, J. A. (2004) Iron−sulfur cluster biosynthesis: Toward an understanding of cellular machinery and molecular mechanism, *Acc. Chem. Res. 37*, 719−725.
4. Johnson, D., Dean, D. R., Smith, A. D., and Johnson, M. K. (2005) Structure, function, and formation of biological iron−sulfur clusters, *Annu. Rev. Biochem. 74*, 247−281.
5. Lill, R., and Mühlenhoff, U. (2005) Iron−sulfur-protein biogenesis in eukaryotes, *Trends Biochem. Sci. 30*, 133−141.
6. Rouault, T. A., and Tong, W.-H. (2005) Iron−sulfur cluster biogenesis and mitochondrial iron homeostasis, *Nat. Rev. Mol. Cell. Biol. 6*, 345−351.
7. Jacobson, M. R., Cash, V. L., Weiss, M. C., Laird, N. F., Newton, W. E., and Dean, D. R. (1989) Biochemical and genetic analysis of the *nifUSVWZM* cluster from *Azotobacter vinelandii*, *Mol. Gen. Genet. 219*, 49−57.
8. Zheng, L., Cash, V. L., Flint, D. H., and Dean, D. R. (1998) Assembly of iron−sulfur clusters. Identification of an *iscSUA-hscBA-fdx* gene cluster from *Azotobacter vinelandii*, *J. Biol. Chem. 273*, 13264−13272.
9. Takahashi, Y., and Tokumoto, U. (2002) A third bacterial system for the assembly of iron−sulfur clusters with homologs in archaea and plastids, *J. Biol. Chem. 277*, 28380−28383.
10. Zheng, L., White, R. H., Cash, V. L., Jack, R. F., and Dean, D. R. (1993) Cysteine desulfurase activity indicates a role for NIFS in metallocluster biosynthesis, *Proc. Natl. Acad. Sci. U.S.A. 90*, 2754−2758.
11. Yuvaniyama, P., Agar, J. N., Cash, V. L., Johnson, M. K., and Dean, D. R. (2000) NifS-directed assembly of a transient [2Fe−2S] cluster within the NifU protein, *Proc. Natl. Acad. Sci. U.S.A. 97*, 599−604.
12. Nishio, K., and Nakai, M. (2000) Transfer of iron−sulfur cluster from NifU to apoferredoxin, *J. Biol. Chem. 275*, 22615−22618.
13. Ollagnier-de-Choudens, S., Mattioli, T., Takahashi, Y., and Fontecave, M. (2001) Iron−sulfur cluster assembly. Characterization of IscA and evidence for a specific functional complex with ferredoxin, *J. Biol. Chem. 276*, 22604−22607.
14. Wu, S.-P., Wu, G., Surerus, K. K., and Cowan, J. A. (2002) Iron−sulfur cluster biosynthesis: Kinetic analysis of [2Fe−2S] cluster transfer from holo ISU to apo Fd: Role of redox chemistry and a conserved aspartate, *Biochemistry 41*, 8876−8885.
15. Wu, S.-P., and Cowan, J. A. (2003) Iron−sulfur cluster biosynthesis. A comparative kinetic analysis of native and cys-substituted ISA-mediated $[2Fe-2S]^{2+}$ cluster transfer to an apoferredoxin target, *Biochemistry 42*, 5784−5791.
16. Wollenberg, M., Berndt, C., Bill, E., Schwenn, J. D., and Seidler, A. (2003) A dimer of the FeS cluster biosynthesis protein IscA from cyanobacteria binds a [2Fe2S] cluster between two protomers and transfers it to [2Fe2S] and [4Fe4S] apo proteins, *Eur. J. Biochem. 270*, 1662−1671.
17. Zheng, L., White, R. H., Cash, V. L., and Dean, D. R. (1994) A mechanism for the desulfurization of L-cysteine catalyzed by the *nifS* gene product, *Biochemistry 33*, 4714−4720.
18. Krebs, C., Agar, J. N., Smith, A. D., Frazzon, J., Dean, D. R., Huynh, B. H., and Johnson, M. K. (2001) IscA, an alternative scaffold for Fe−S cluster biosynthesis, *Biochemistry 40*, 14069−14080.
19. Olson, J. W., Agar, J. N., Johnson, M. K., and Maier, R. J. (2000) Characterization of the NifU and NifS Fe−S cluster formation proteins essential for the viability of *Helicobacter pylori*, *Biochemistry 39*, 16213−16219.
20. Ali, V., Shigeta, Y., Tokumoto, U., Takahashi, Y., and Nozaki, T. (2004) An intestinal parasitic protist, *Entamoeba histolytica*, possesses a non-redundant nitrogen fixation-like system for iron−sulfur cluster assembly under anaerobic conditions, *J. Biol. Chem. 279*, 16863−16874.
21. Takahashi, Y., and Nakamura, M. (1999) Functional assignment of the ORF2-*iscS-iscA-hscB-hscA-fdx*-ORF3 gene cluster involved in the assembly of Fe−S clusters in *Escherichia coli*, *J. Biochem. 126*, 917−926.
22. Silberg, J. J., Hoff, K. G., Tapley, T. L., and Vickery, L. E. (2001) The Fe/S assembly protein IscU behaves as a substrate for the molecular chaperone Hsc66 from *Escherichia coli*, *J. Biol. Chem. 276*, 1696−1700.
23. Hoff, K. G., Ta, D. T., Tapley, T. L., Silberg, J. J., and Vickery, L. E. (2002) Hsc66 substrate specificity is directed toward a discrete region of the iron−sulfur cluster template protein IscU, *J. Biol. Chem. 277*, 27353−27359.
24. Hoff, K. G., Cupp-Vickery, J. R., and Vickery, L. E. (2003) Contributions of the LPPVK motif of the iron−sulfur template protein IscU to interactions with the Hsc66−Hsc20 chaperone system, *J. Biol. Chem. 278*, 37582−37589.
25. Cupp-Vickery, J. R., Peterson, J. C., Ta, D. T., and Vickery, L. E. (2004) Crystal structure of the molecular chaperone HscA substrate binding domain complexed with the IscU recognition peptide ELPPVKIHC, *J. Mol. Biol. 342*, 1265−1278.
26. Mühlenhoff, U., Gerber, J., Richhardt, N., and Lill, R. (2003) Components involved in assembly and dislocation of iron−sulfur clusters on the scaffold protein Iscu1p, *EMBO J. 22*, 4815−4825.
27. Patzer, S. L., and Hantke, K. (1999) SufS is a NifS-like protein, and SufD is necessary for stability of the [2Fe−2S] FhuF protein in *Escherichia coli*, *J. Bacteriol. 181*, 3307−3309.
28. Loiseau, L., Ollagnier-de-Choudens, S., Nachin, L., Fontecave, M., and Barras, F. (2003) Biogenesis of Fe−S cluster by the bacterial Suf system. SufS and SufE form a new type of cysteine desulfurase, *J. Biol. Chem. 278*, 38352−38359.
29. Outten, F. W., Wood, M. J., Muñoz, F. M., and Storz, G. (2003) The SufE protein and the SufBCD complex enhance SufS cysteine desulfurase activity as part of a sulfur transfer pathway for Fe−S cluster assembly in *E. coli*, *J. Biol. Chem. 278*, 45713−45719.
30. Ramelot, T. A., Cort, J. R., Goldsmith-Fischman, S., Kornhaber, G. J., Xiao, R., Shastry, R., Acton, T. B., Honig, B., Montelione, G. T., and Kennedy, M. A. (2004) Solution NMR structure of the iron−sulfur cluster assembly protein U (IscU) with zinc bound at the active site, *J. Mol. Biol. 344*, 567−583.
31. Goldsmith-Fischman, S., Kuzin, A., Edstrom, W. C., Benach, J., Shastry, R., Xiao, R., Acton, T. B., Honig, B., Montelione, G. T., and Hunt, J. F. (2004) The SufE sulfur-acceptor protein contains a conserved core structure that mediates interdomain interactions in a variety of redox protein complexes, *J. Mol. Biol. 344*, 549−565.
32. Ollagnier-de-Choudens, S., Lascoux, D., Loiseau, L., Barras, F., Forest, E., and Fontecave, M. (2003) Mechanistic studies of the SufS−SufE cysteine desulfurase: Evidence for S transfer from SufS to SufE, *FEBS Lett. 555*, 263−267.
33. Ollagnier-de-Choudens, S., Nachin, L., Sanakis, Y., Loiseau, L., Barras, F., and Fontecave, M. (2003) SufA from *Erwinia chrysanthemi*. Characterization of a scaffold protein required for iron−sulfur cluster assembly, *J. Biol. Chem. 278*, 17993−18001.
34. Mansy, S. S., Wu, G., Surerus, K. K., and Cowan, J. A. (2002) Iron−sulfur cluster biosynthesis. *Thermatoga maritima* IscU is a structured iron−sulfur cluster assembly protein, *J. Biol. Chem. 277*, 21397−21404.

35. Agar, J. N., Zheng, L., Cash, V. L., Dean, D. R., and Johnson, M. K. (2000) Role of the IscU protein in iron−sulfur cluster biosynthesis: IscS-mediated assembly of a $[Fe_2S_2]$ cluster in IscU, *J. Am. Chem. Soc. 122*, 2136−2137.
36. Wu, G., Mansy, S. S., Hemann, C., Hille, R., Surerus, K. K., and Cowan, J. A. (2002) Iron−sulfur cluster biosynthesis: Characterization of *Schizosaccharomyces pombe* Isa1, *J. Biol. Inorg. Chem. 7*, 526−532.
37. Morimoto, K., Nishio, K., and Nakai, M. (2002) Identification of a novel prokaryotic HEAT-repeats-containing protein which interacts with a cyanobacterial IscA homolog, *FEBS Lett. 519*, 123−127.
38. Bertini, I., Cowan, J. A., del Bianco, C., Luchinat, C., and Mansy, S. S. (2003) *Thermotoga maritima* IscU. Structural characterization and dynamics of a new class of metallochaperone, *J. Mol. Biol. 331*, 907−924.
39. Mansy, S. S., Wu, S.-P., and Cowan, J. A. (2004) Iron−sulfur cluster biosynthesis. Biochemical characterizarion of the conformational dynamics of *Thermatoga maritima* IscU and the relevance fo cellular cluster assembly, *J. Biol. Chem. 279*, 10469−10475.
40. Agar, J. N., Krebs, B., Frazzon, J., Huynh, B. H., Dean, D. R., and Johnson, M. K. (2000) IscU as a scaffold for iron−sulfur cluster biosynthesis: Sequential assembly of [2Fe−2S] and [4Fe−4S] clusters in IscU, *Biochemistry 39*, 7856−7862.
41. Urbina, H. D., Silberg, J. J., Hoff, K. G., and Vickery, L. E. (2001) Transfer of sulfur from IscS to IscU during Fe/S cluster assembly, *J. Biol. Chem. 276*, 44521−44526.
42. Wu, G., Mansy, S. S., Wu, S.-P., Surerus, K. K., Foster, M. W., and Cowan, J. A. (2002) Characterization of an iron−sulfur cluster assembly protein (ISU1) from *Schizosaccharomyces pombe*, *Biochemistry 41*, 5024−5023.
43. Foster, M. W., Mansy, S. S., Hwang, J., Penner-Hahn, J. E., Surerus, K. K., and Cowan, J. A. (2000) A mutant human IscU protein contains a stable $[2Fe-2S]^{2+}$ center of possible functional significance, *J. Am. Chem. Soc. 122*, 6805−6806.
44. Yabe, T., Morimoto, K., Kikuchi, S., Nishio, K., Terashima, I., and Nakai, M. (2004) The arabidopsis chloroplast NifU-like protein CnfU, which can act as an iron−sulfur cluster scaffold protein, is required for the biogenesis of ferredoxin and photosystem I, *Plant Cell 16*, 993−1007.
45. Tong, W.-H., Jameson, G. N. L., Huynh, B. H., and Rouault, T. A. (2003) Subcellular compartmentalization of human Nfu, an iron−sulfur cluster scaffold protein and its ability to assemble a [4Fe−4S] cluster, *Proc. Natl. Acad. Sci. U.S.A. 100*, 9762−9767.
46. Agar, J. N., Yuvaniyama, P., Jack, R. F., Cash, V. L., Smith, A. D., Dean, D. R., and Johnson, M. K. (2000) Modular organization and identification of a mononuclear iron-binding site within the NifU protein, *J. Biol. Inorg. Chem. 5*, 167−177.
47. Dos Santos, P. C., Smith, A. D., Frazzon, J., Cash, V. L., Johnson, M. K., and Dean, D. R. (2004) Iron−sulfur cluster assembly: NifU-directed activation of the nitrogenase Fe-protein, *J. Biol. Chem. 279*, 19705−19711.
48. Fu, W., Jack, R. F., Morgan, T. V., Dean, D. R., and Johnson, M. K. (1994) *nifU* gene product from *Azotobacter vinelandii* is a homodimer that contains two identical [2Fe−2S] clusters, *Biochemistry 33*, 13455−13463.
49. Garg, R. P., Vargo, C. J., Cui, X., and Kurtz, D. M., Jr. (1996) A [2Fe−2S] protein encoded by an open reading frame upstream of the *E. coli* bacterioferritin gene, *Biochemistry 35*, 6297−6301.
50. Quail, M. A., Jordan, P., Grogan, J. M., Butt, J. N., Lutz, M., Thomson, A. J., Andrews, S. C., and Guest, J. R. (1996) Spectroscopic and voltammetric characterization of the bacterioferritin-associated ferredoxin from *Escherichia coli*, *Biochem. Biophys. Res. Commun. 229*, 635−642.
51. Brown, R. E., Jarvis, K. L., and Hyland, K. J. (1989) *Anal. Biochem. 180*, 136−139.
52. Fish, W. W. (1988) Rapid colorimetric micromethod for the quantitation of complexed iron in biological samples, *Methods Enzymol. 158*, 357−364.
53. Ugulava, N. B., Gibney, B. R., and Jarrett, J. T. (2001) Biotin synthase contains two distinct iron−sulfur cluster binding sites: Chemical and spectroelectrochemical analysis of iron−sulfur cluster interconversions, *Biochemistry 40*, 8343−8351.
54. Ravi, N., Bollinger, J. M., Huynh, B. H., Edmondson, D. E., and Stubbe, J. (1994) Mechanism of assembly of the tyrosyl radical-diiron(III) cofactor of *E. coli* ribonucleotide reductase. 1. Mössbauer characterization of the diferric radical precusor, *J. Am. Chem. Soc. 116*, 8007−8014.
55. Schilke, B., Voisine, C., Beinert, H., and Craig, E. (1999) Evidence for a conserved system for iron metabolism in the mitochondria of *Saccharomyces cerevisiae*, *Proc. Natl. Acad. Sci. U.S.A. 96*, 10206−10211.
56. Léon, S., Touraine, B., Ribot, C., Briat, J.-F., and Lobréaux, S. (2003) Iron−sulfur cluster assembly in plants: Distinct NFU proteins in mitochondria and plastids from *Arabidopsis thaliana*, *Biochem. J. 371*, 823−830.
57. Ollagnier-de-Choudens, S., Sanakis, Y., and Fontecave, M. (2004) SufA/IscA: Reactivity studies of a class of scaffold proteins involved with [Fe−S] cluster assembly, *J. Biol. Inorg. Chem. 9*, 828−838.
58. Agar, J. N., Dean, D. R., and Johnson, M. K. (2003) Iron−sulfur cluster biosynthesis, in *Biochemistry and Physiology of Anaerobic Bacteria* (Ljungdahl, L. G., Adams, M. W. W., Barton, L. L., Ferry, J. G., and Johnson, M. K., Eds.) pp 46−66, Springer-Verlag, New York.

BI051257I